TURUN YLIOPISTO
UNIVERSITY OF TURKU

Lessons learned from combining cellulose films with perovskite solar cells

Joaquín Valdez García

TURUN YLIOPISTON JULKAISUJA – ANNALES UNIVERSITATIS TURKUENSIS
SARJA - SER. F OSA - TOM. 72 | TECHNICA - INFORMATICA | TURKU 2026

TURUN
YLIOPISTO
UNIVERSITY
OF TURKU

LESSONS LEARNED FROM COMBINING CELLULOSE FILMS WITH PEROVSKITE SOLAR CELLS

Joaquín Valdez García

TURUN YLIOPISTON JULKAISUJA – ANNALES UNIVERSITATIS TURKUENSIS
SARJA – SER. F OSA – TOM. 72 | TECHNICA – INFORMATICA | TURKU 2026

University of Turku

Faculty of Technology
Department of Mechanical and Materials Engineering
Materials Engineering
Doctoral programme of Technology

Supervised by

Professor Kati Miettunen
University of Turku

Dr. Mahboubeh Hadadian
University of Turku

Reviewed by

Assistant Professor Peter Olsén
Linköping University

Professor Hele Savin
Aalto University

Opponent

Dr. Sjoerd Veenstra
Netherlands Organization for Applied
Scientific Research (TNO)

The originality of this publication has been checked in accordance with the University of Turku quality assurance system using the Turnitin OriginalityCheck service.

Cover Image: Mikael Nyberg, University of Turku

ISBN 978-952-02-0522-5 (PRINT)
ISBN 978-952-02-0523-2 (PDF)
ISSN 2736-9390 (Print)
ISSN 2736-9684 (Online)
Grano Oy, Turku, Finland 2026

A todos los que me han brindado apoyo, cariño, y amor:
una vida no me bastaría para agradecerles

UNIVERSITY OF TURKU
Faculty of Technology
Department of Mechanical and Materials Engineering
Materials Engineering
JOAQUÍN VALDEZ GARCÍA: Lessons learned from combining cellulose films with perovskite solar cells
Doctoral Dissertation, 000 pp.
Doctoral Programme in Technology
January 2026

ABSTRACT

Solar energy is one of the most promising renewable energy sources, yet increasing solar cell production raises concerns about end-of-life recycling. Currently, solar panel recycling remains challenging due to the difficulty to separate valuable materials from glass and encapsulants, making device redesign essential. This thesis explores cellulose as a substrate that supports the fabrication of perovskite solar cells.

The research assessed cellulose films in terms of their compatibility with perovskite solar cells, mainly their optics, surface morphology, mechanical properties. After optimizing the transparency, surface roughness, and tensile strength of unmodified cellulose nanofibrils films, different nanocellulose grades were tested alongside, yet, they were deemed too rough to be used as substrates. Cellulose nanocrystal films reached surface roughness comparable to conventional substrates, though with reduced flexibility. Combining nanocrystals with nanofibrils improved flexibility and moisture resistance, but increased surface roughness. Additionally, while highly transparent at normal incidence, nanocellulose films exhibited increased reflectivity at angles above 45° due to light scattering by cellulose fibrils.

In the traditional perovskite solar cell fabrication route, the bottom electrode is deposited on the substrate, then etched and patterned for electrically isolated sections (i.e., pixels). To accommodate cellulose substrates, a customizable measuring apparatus was developed to circumvent this step. This tool helped to prove that devices made on non-patterned unetched substrates devices work as well as those made on etched ones, enabling early-stage characterization on cellulose films.

This work concludes with the creation of a methodology for the fabrication of more sustainable solar cells through the combination of robust cellulose substrates and alternative perovskite solar cell fabrication methods. These findings contribute to the development of truly renewable energy sources.

KEYWORDS: Perovskite, solar cell, cellulose, flexible, recycling, sustainability

TURUN YLIOPISTO
Teknillinen tiedekunta
Kone- ja materiaalitekniikan laitos
Materiaalitekniikka
Joaquín Valdez García: Lessons learned from combining cellulose films with perovskite solar cells
Väitöskirja, 000 s.
Teknologian tohtoriohjelma (DPT)
Tammikuu 2026

TIIVISTELMÄ

Aurinkoenergia on yksi lupaavimmista uusiutuvan energian lähteistä, mutta aurinkokennojen kierrätys on edelleen haastavaa. Tämä johtuu erityisesti siitä, että kennojen materiaalien erottelu on vaikeaa. Uusilla kennorakenteilla arvokkaiden materiaalien talteenottoa voitaisiin kehittää. Tässä työssä tarkastellaan biopohjaisten materiaalien, erityisesti selluloosan, hyödyntämistä aurinkokennojen valmistuksessa.

Tutkimuksessa arvioitiin selluloosakalvojen sopivuutta perovskiitti-aurinkokennoihin, painottaen optiikkaa, pinnan morfologiaa ja mekaanisia ominaisuuksia. Muokkaamattomien nanofibrillikalvojen läpinäkyvyyden, karheuden ja mekaanisen kestävyyden optimoinnin lisäksi testattiin erilaisia nanoselluloosalaatuja, mutta nämä osoittautuivat liian karkeiksi. Nanokiteistä valmistetut kalvot saavuttivat tavallisiin substraatteihin verrattavan karheuden, tosin vähäisemmällä joustavuudella. Nanokiteiden yhdistäminen nanofibrilleihin paransi kalvojen joustavuutta ja kosteudenkestävyyttä, mutta lisäsi pinnan karheutta. Lisäksi havaittiin, että vaikka nanoselluloosakalvot ovat tavanomaisesti hyvin läpinäkyviä, niiden heijastavuus kasvaa yli 45° kulmissa johtuen fibrillien aiheuttamasta valon sironnasta.

Perinteisesti perovskiittikenno valmistetaan kerrostamalla elektrodi substraatille, minkä jälkeen se etsataan halutun sähköisesti erotellun jaon, ns. pikselöinnin, saavuttamiseksi. Tämän vaiheen kiertämiseksi kehitettiin muokattavissa oleva mittalaite. Tämä auttoi todistamaan, että ei-kuvioiduilla ja etsaamattomilla substraateilla tehdyt laitteet toimivat yhtä hyvin etsatut, mikä mahdollistaa varhaisessa kehitysvaiheessa olevien selluloosakalvojen karakterisoinnin.

Työn viimeinen osa esittelee menetelmiä ympäristöystävällisempien aurinkokennojen valmistukseen yhdistämällä vankkoja selluloosasubstraatteja ja vaihtoehtoisia perovskiittikennojen valmistusmenetelmiä. Nämä tulokset edistävät aidosti uusiutuvien energianlähteiden kehittämistä.

AVAINSANAT: Perovskiitti, aurinkokenno, selluloosa, joustava, kierrätys, kestävyys

Acknowledgements

Writing this book did not take very long, but reaching the point where I was able to do so took a lifetime. I have often been told that most doctoral students do not feel proud of their theses, which is understandable: you graduate and reach a stage in your career where you realize how much there still is to learn, you may lack confidence in your skills, and you become acutely aware of the level of expertise required in your field. For this reason, I am deeply grateful to those who reminded me that this book is, in fact, a significant achievement. It represents not only my scientific work, but also the culmination of years of support, encouragement, and guidance.

First and foremost, I am grateful to my supervisor, Prof. Kati Miettunen, for welcoming me into her research group and guiding my doctoral studies. Her encouragement and support were indispensable to the completion of my degree. I am also deeply thankful to my second supervisor, Dr. Mahboubeh Hadadian, for constantly reminding me not to be discouraged when experiments did not go as planned and for teaching me most of the practical knowledge I have about perovskites. I also thank the pre-examiners of my thesis, Prof. Peter Olsén and Prof. Hele Savin, for their insightful and valuable feedback. Likewise, I am grateful to my opponent, Dr. Sjoerd Veenstra, for his engagement with my work and his much-appreciated expert perspective. Financial support from the Finnish Cultural Foundation, the Research Council of Finland, the University of Turku Graduate School, the Turku University Foundation, the Viperlab project, and especially the Magnus Ehrnrooth Foundation is also gratefully acknowledged.

This work is the result of extensive collaboration. I am thankful to my collaborators Prof. Joice Kaschuk, Prof. Tiffany Abitbol, and Dr. Matteo Hirsch for teaching me so much about cellulose. I also thank Prof. Paola Vivo and her students, Noora Lamminen and Paavo Mäkinen, for their assistance with our perovskite research. In addition, I am grateful to Dr. Riikka Suhonen and Dr. Marja Välimäki for their expert input and valuable contributions to our work.

I would like to extend my sincere gratitude to the entire SEMS team, past and present, as well as to the Mechanical and Materials Engineering Department at the University of Turku, for their continuous support and the shared time along the way.

In particular, I thank my colleagues and friends Dr. Rustem Nizamov and Dr. Manish Kumar for brightening my weeks and teaching me how comforting a cup of coffee can be, as well as Dr. Konstantinos Konstatinou and Oskar Tuomi for our innumerable fancy lunches. I am also grateful to Mikael Nyberg and the support team—Helen Salminen, Akseli Nykänen, and Teemu Hynnä—for assisting me and the entire department throughout these years. Beyond my department, I thank Dr. Mikko Salomäki from the Chemistry Department for teaching me how to use the AFM, an essential instrument in my research, and Dr. Ermei Mäkilä and Dr. Saari Granroth from Physics for their help with the shared infrastructure in our building. From Åbo Akademi, I thank Prof. Ronald Österbacka, Dr. Jan-Henrik Smått, and Staffan Dahlström for their continued support in our perovskite solar cell efforts. I am also grateful to Dr. Stéphane Cros and Dr. Matthieu Manceau for hosting me at their institute and helping me achieve the goal of merging cellulose and perovskite technologies.

I am especially thankful to all my friends—those back home, those abroad, and those I met in Turku during my studies—for their friendship. To my friends in Turku, you truly made it feel like home, and I am deeply grateful for having met you. In no particular order, I thank Chandler, Raychel, Santeri, Denis, Barbara, Antti, Marek, Claudia, Samppa, Merve, Tuulia, Paola, Magda, Karo, Tsege, Yigit, Daniel, Marta, Marcelo, Kat, Petar, Sai, Octav, Ian, Aryane, Sofia, Matti, Ricardo, Iliana, Bertram, Azael, Joselyne, Eddiel, Patricia, Julio, and Catalina. If I have unintentionally omitted anyone, please forgive me—writing this section is deeply emotional, and I cannot help missing some names in the commotion.

Finally, I thank my family. I truly lack the words to express how much I owe you. I would not have come this far without your unwavering support and sacrifice, and I promise not to let you down. You are constantly in my prayers.

January 7, 2026
Joaquín Valdez García

Table of Contents

Abbreviations

AFM	Atomic force microscopy
CBM	Conduction band minimum
CTL	Charge transport layer
DP	Degree of polymerization
DS	Degree of substitution
EA	Electron affinity
ETL	Electron transport layer
FOM	Figure-of-merit
HTL	Hole transport layer
IE	Ionization energy
IV	Current - voltage
JV	Current density – voltage
OSC	Organic solar cell
OSSP	One-step solution process
OTR	Oxygen transmission rate
PID	Proportional-integral-derivative
PSC	Perovskite solar cell
PV	Photovoltaic
R2R	Roll-to-roll
SEM	Scanning electrode microscopy
TCO	Transparent conductive oxide

TEM	Transmission electron microscopy
TSSP	Two-step solution process
UV-O_3	Ultraviolet-ozone
VBM	Valence band maximum
WVTR	Water vapor transmission rate

Materials

ACN	Acetonitrile
CB	Chlorobenzene
CNC	Cellulose nanocrystals
CNF	Cellulose nanofibrils
DMF	Dimethyl formamide
DMSO	Dimethyl sulfoxide
EC	Ethyl cellulose
ETPTA	Ethoxylated trimethylolpropane triacrylate
EVA	Ethylene-vinyl acetate
FA	Formamidinium
FK209	tris(2-(1*H*-pyrazol-1-yl)-4-*tert*-butylpyridine)cobalt(III) tri[bis(trifluoromethane)sulfonimide]
FTO	Fluorinated tin oxide
ITO	Indium tin oxide
LiTFSI	Bis(trifluoromethylsulfonyl)amine lithium salt
MA	Methylammonium
NiO_x	Nickel oxide
PEN	Polyethylene naphthalate
PET	Polyethylene terephthalate
SnO_2	Tin oxide

Spiro-OMeTAD $N^2,N^2,N^{2'},N^{2'},N^7,N^7,N^{7'},N^{7'}$-octakis(4-methoxyphenyl)-9,9′-spirobi[9H-fluorene]-2,2′,7,7′-tetramine

TiO_2 Titanium dioxide or titania

ZnO Zinc oxide

Symbols

CTE	Coefficient of thermal expansion
FF	Fill factor
I_{SC}	Short-circuit current
J_{SC}	Short-circuit current density
PCE	Power conversion efficiency
R_{Rec}	Recombination resistance
R_S	Series resistance
V_{OC}	Open-circuit voltage

List of Original Publications

This dissertation is based on the following original publications, which are referred to in the text by their Roman numerals:

I Kati Miettunen, Mahboubeh Hadadian, **Joaquin Valdez Garcia**, Alicja Lawrynowicz, Elena Akulenko, Orlando Rojas, Micheal Hummel, Jaana Vapaavuori. Bio-based materials for solar cells. *WIREs Energy and Environment*, 2024; 1: e508.
https://doi.org/10.1002/wene.508

II Joice Kaschuk, Yazan Al Haj, **Joaquin Valdez Garcia**, Aleksi Kamppinen, Orlando Rojas, Tiffany Abitbol, Kati Miettunen, Jaana Vapaavuori. Processing factors affecting roughness, optical and mechanical properties of nanocellulose films for optoelectronics. *Carbohydrate polymers*, 2024; 332: 121877.
https://doi.org/10.1016/j.carbpol.2024.121877

III **Joaquin Valdez Garcia**, Anna Boding, Xuan Yang, Rustem Nizamov, Michael S. Reid, Kristina Junel, Kati Miettunen, Tiffany Abitbol, Joice Kaschuk. Multifunctional nanocellulose hybrid films: From packaging to photovoltaics. *International Journal of Biological Macromolecules*, 2025; 292: 139203.
https://doi.org/10.1016/j.ijbiomac.2024.139203

IV **Joaquin Valdez Garcia**, Mahboubeh Hadadian, Rustem Nizamov, Paavo Mäkinen, Noora Lamminen, Paola Vivo, Kati Miettunen. Simplifying perovskite solar cell fabrication for materials testing: how to use unetched substrates with the aid of a three-dimensionally printed cell holder. *Royal Society Open Science*, 2025; 11: 241012.
https://doi.org/10.1098/rsos.241012

V **Joaquin Valdez Garcia**, Mahboubeh Hadadian, Vidushi Aggarwal, Sirius Yli-Paavola, Joice Kaschuk, Riikka Suhonen, Marja Valimäki, Kati Miettunen. Combining cellulose substrates and perovskites in sustainable solar cells is possible: a systematic literature review offering realistic solutions. *Green Chemistry*, Accepted January 2026

Declaration of AI use

In preparing this work, OpenAI's ChatGPT was used solely to correct grammar and spelling and to improve readability in limited instances. No AI tools were used to develop research concepts, analyze data, or draw conclusions.

Author's contribution

In **Publication I**, the doctoral candidate reviewed the current literature on cellulose-based materials and analyzed their suitability as perovskite solar cell substrates, writing the corresponding article sections.

In **Publications II and III**, the doctoral candidate analyzed cellulose films through angle dependent transmittance measurements and atomic force microscopy, and compared their properties to currently-used solar cell substrate materials. In these two articles, the doctoral candidate wrote specific manuscript sections related sections to his results, as well as producing and editing some of the figures. All cellulose samples featured in these publications were prepared by internal and external collaborators.

In **Publication IV**, the doctoral candidate conceptualized the design of a characterization holder for solar cells, and fabricated and characterized perovskite solar cells alongside external collaborators to prove the main hypothesis of the article. In this publication, the doctoral candidate wrote the majority of the manuscript.

In **Publication V**, the doctoral candidate wrote an extensive literature review establishing a methodology to combine cellulose substrates and perovskite solar cell through alternative fabrication methods.

1 Introduction

1.1 Contextual overview

Reliance on fossil fuels has had many negative impacts on the environment and the world economy: air pollution, water pollution due to oil spillages, energy market volatility, armed conflicts over oil and gas rich areas, but above all else, the release of greenhouse gases into the atmosphere responsible for global climate change [1], [2], [3], [4]. Energy demand is expected to increase, and unless we curb the negative effects of fossil fuels usage, we will be faced with many environmental and political crises [5].

New technologies are required to satisfy the world's need for clean energy. Solar energy appears as one of the most promising alternative sources. An almost unlimited energy source, sunlight can be converted into electricity through photovoltaic (PV) devices [6]. To date, the global renewable energy share of electricity capacity is around 43.2%, which includes hydropower, wind, solar, biofuels, among others. This amounts to around 3.87 TW of installed power generation of which 1.4 TW correspond to photovoltaic solar energy [7]. As the demand for clean energy increases, so does the fabrication of PV modules – in 2024 700 GW of silicon solar panels were produced [8], and it is projected that the manufacturing capacity could reach 2.5 TWp by 2030 [9]. Silicon solar module fabrication is mostly concentrated in China, owning 95% of the new facilities installed in 2022 [10], and module prices reached the lowest level ever at 0.096 USD/Watt in 2024 [11].

As solar module prices drop and solar energy is more and more adopted across the world, it is expected that a high volume of solar modules will be produced to tackle climate change. An often-overlooked problem with solar modules is their circular economy. Silicon technology dominates the photovoltaic market with more than 90% of the installed capacity, and with an average lifetime of 25 years, our recycling capacity is not enough to deal with this problem [12]. Modules are built by encapsulating the components between rigid layers of glass and plastic, sealed with a polymer, usually ethylene vinyl acetate (EVA), and encased in an aluminum frame. This structure makes modules very resistant to the outdoors, however, this also

complicates their recycling, interrupting their circular economy. The current recycling process for solar modules consists in separating the aluminum frame and junction box from the module, removing the EVA, and finally removing the silicon wafers and recover the metals used for internal connections [12], [13], however, this method has yet to be adopted at an industrial scale.

Most of the value of a solar module lies in its internal components. Silver used in the internal connections is a scarce and precious resource, and if the current trends continue, it is expected that between 85 to 98% of the total silver reserves will be used to manufacture solar modules [14]. Furthermore, at the current mining rate, it is expected that the global silver reserves will be depleted in less than 20 years [15]. The silicon wafers, while made from a very abundant material, require high energy intensive processes to achieve the necessary purity level for solar cells. Unfortunately, recovering silicon wafers from modules has proven to be quite challenging. Typically, modules are mechanically shredded and then processed to recover valuable materials. To avoid damaging the wafer, a chemical delamination approach is preferred, although it has been observed that there are still encapsulant residues on the wafer that need to be removed via pyrolysis [16]. Whereas silicon is the most used PV technology, its recycling complications encourage us to look elsewhere for more sustainable alternatives.

Second and third generation solar cell technologies have started being fabricated on flexible synthetic substrates, i.e. polyethylene terephthalate (PET) and polyethylene naphthalate (PEN). These substrates have several advantages: they are cheap, have very smooth surfaces, are highly transparent, and are well-known industrial materials [17], [18], [19]. Yet, one big issue is their fossil origin. Although synthetic thermoplastic polymers can be recycled, they degrade on every cycle and require new material to be introduced in the process [20], [21]. Ideally, the substrate and the electrode attached to it, normally indium tin oxide (ITO), should be recovered to be reused in new devices, but unfortunately, ITO can present cracks due do bending [22]. The most likely approach for recycling those devices after removing the encapsulant would be incinerating them to remove the polymer substrate and recover the valuable materials. A more convenient solution would be to use a more sustainable material that does not produce as much emissions and waste as synthetic polymer.

Cellulose has surged as an interesting bio-based alternative to synthetic polymer substrates in solar devices. As the most abundant biopolymer on the planet, cellulose can be obtained from a variety of renewable sources like cotton, trees, and even bacteria [23]. Cellulose transparent films have raised interest in the scientific community due to the possibility of making printable devices on a more sustainable substrate [24], [25], [26] – thanks to its transparency it can allow light to reach the active components of solar cells. An important limitation of cellulose films is their

low thermal stability. Unmodified cellulose films flexibility decreases with water loss from inside the bulk when heated between 75 and 120 °C, but their complete thermal degradation is around 300 °C, depending on the type of cellulose [27], [28], [29]. In contrast, PET and PEN mechanical integrity are compromised after their glass transition temperatures, between 69 °C and 120 °C [30]. As such, cellulose cannot resist certain deposition methods and annealing temperatures commonly used, i.e., highly conductive ITO and fluorinated tin oxide (FTO) annealing temperatures between 350 and 500 °C [31], [32], although it can resist higher temperatures than PET and PEN. Therefore, its adoption as a substrate is restricted to low-temperature processed solar cells.

One of the most promising emerging technologies in PV are Perovskite Solar Cells (PSCs). While PSCs suffer from low stability, their entry into the solar module market is seen as imminent due to their rapid increase in power conversion efficiency (*PCE*) year by year. Characterized by a relatively easy, low temperature and low-cost fabrication than their silicon counterparts, PSCs have shown an incredible increase in efficiency [33]. Unlike silicon solar cells where the silicon wafer is treated to become photoactive, PSCs are made by sequentially depositing thin films with different roles, such as electrodes, transport and passivation layers, and photoactive perovskite materials. PSCs had a meager 3.8% *PCE* when first used by Miyasaka et al. in 2009 [34], and in just 15 years they have had an amazing improvement reaching 26.7% [35]. Its ability to be processed at around 100 °C naturally pairs it with cellulose to make easily recyclable and high-efficiency solar cells.

There are various issues in combining cellulose and PSCs. As mentioned before, cellulose burning limits the fabrication temperatures, as some layers require annealing steps around 400 °C in mesoporous architectures. Furthermore, depending on the type of cellulose, it can disperse in the solvents used during the fabrication. Moreover, films made from the same cellulose material can present different surface morphologies, optical and mechanical properties, and these properties can be consequences of changing a handful of variables during casting. From how concentrated the cellulose is in the solution, how fast it dries, the molecular size of the cellulose chains, the material and surface of the container where the film is drying, to how much air is dissolved in the solution; all these variables affect the properties of the films [36].

This thesis focuses on the adaptation of nanocellulose as viable substrate for PSCs. In it I discuss how nanocellulose processing affects the characteristics of cellulose films and how it would affect the fabrication of PSCs and other optoelectronic devices. Later on, I discuss experimental results about the adaptation of characterization techniques to PSCs fabricated on unetched substrates where the

electrode is unpatterned. Finally, there is an exhaustive review on the fabrication of PSCs on cellulose films.

1.2 Objectives and scope

The main idea of this thesis is the tuning both cellulose films as substrates and the PSC fabrication methods. It aims to discuss the requirements for a proper substrate for PSCs by examining them with multiple characterization techniques. Since cellulose films are new substrates materials in photovoltaics, there is still a large knowledge gap that needs to be bridged before adopting this new technology. Understanding the inherent limits of the material via different processing routes will delineate clearer guidelines on how to adapt bio-based materials into PV devices. The main topic is divided into three research questions:

1. How photovoltaics can benefit from bio-based materials?
2. How nanocellulose processing affects the properties required for films to be used as solar cell substrates?
3. How do PSCs and nanocellulose have to be adapted to work together?

The first question relates to the importance of introducing or replacing existing materials in PV for bio-based alternatives. If high efficiencies and stabilities of new generation solar cells can be maintained, switching to bio-based materials has the potential of increasing PV's sustainability, its recyclability, and lowering its cost. What components can be replaced, what are the alternative's limitations and advantages, and how they impact the device sustainability are all questions that need to be discussed thoroughly.

The second question concerns the methods used to produce the cellulose films and how these affected the final results. While cellulose is simply a chain of glucose units, many factors come into play that define resulting film. Important factors include how many glucose units form the chain (called the degree of polymerization), how the -OH functional groups have been changed, how hydrogen bonds of different chains interact, how the films were dried, etc. Therefore, the understanding of what properties can the cellulose films have and how they can be achieved should be given great importance.

The last question deals with how the fabrication process of PSCs can affect the substrate, how the process can be adapted to work with cellulose, or how can the cellulose be modified to withstand the process. Regular fabrication methods are not yet adapted to work with cellulose, as it is a new material used in PV. An electrode material that can be fabricated at low temperatures should be selected. If the solvents used in the process cannot be changed, only cellulose that can resist these solvents

should be considered. **Table 1** shows which publications answer which research questions.

Table 1. Where each research question is discussed in the publications included in this thesis

RESEARCH QUESTION	PUBLICATION I	PUBLICATION II	PUBLICATION III	PUBLICATION IV	PUBLICATION V
RQ1	X	X	X		X
RQ2		X	X		X
RQ3				X	X

This thesis focuses on adapting the surface roughness of the films to similar values to those of glass, PET, and PEN while maintaining good optical and mechanical properties, and what types of cellulose can resist the fabrication process of PSCs.

1.3 Thesis outline

This thesis is based on five publications and they are found in the list of publications at the beginning of this work. The first part of Chapter 2 discusses cellulose more thoroughly, the different treatments cellulose undergoes, how films are made, and what factors affect them. The second part deals with the operation principles of PSCs, their fabrication and the factors that affect their functioning during fabrication, as well as the methods used to fabricate and characterize the films and solar cells made throughout the five publications. Chapter 3 describes the methods used in all publications.

The results of the publications are discussed in Chapter 4. This chapter is subdivided in three sections according to the research questions described in section 1.2. The first research question is answered mostly by **Publication I**, with small contributions from **Publication II, III and V**, as they directly address the integration of bio-based materials in PV. **Publications II, III, and V** focus on the modification and application of cellulose for photovoltaic purposes, addressing the second research question. Finally, the answer to the third research question is based around **Publication IV and V**, as they directly engage with the fabrication and characterization of PSCs. **Publication V** contributes to answer all the research questions, as it is the culmination of this thesis.

Chapter 5 ends this thesis with a discussion of the results and suggestions for further research. The publications included in the thesis are reprinted after this section.

2 Background

2.1 Cellulose

Cellulose is the most abundant biopolymer in the planet, and it has been used by humanity throughout history in textiles, paper, food additives, construction, and other applications [37]. It is a structural part of all plant life, sustainable, widely available, non-toxic, and cheap. Cellulose is primarily derived from three sources: cotton, bacteria, and wood. Cotton is the purest source of cellulose, containing only minor percentages of fats and waxes. While its purity makes cotton the ideal source for textiles, its cultivation is highly water intensive [38]. Pure cellulose can also be produced by certain types of bacteria, although this is approach is quite inefficient and expensive at the moment [39]. Cellulose can be found in wood in different percentages depending on the tree, mixed with hemicellulose and lignin (**Figure 1**) [40].

From an optoelectronics perspective, cellulose has the interesting capability of forming transparent films that can be used as substrates for flexible and printed electronics. Typically, cellulose is not thought as transparent, but as an opaque material. It has a refractive index different from air, and as a biopolymer, it forms long fibers that in turn create porous structures. These structures scatter light to such a degree that the bulk material appears opaque [41]. Cellulose first needs to be broken down and then reconstituted to form transparent films. This requires a more in-depth understating of what cellulose is and how it can be modified. Hemicellulose and lignin have also been used to make films, cellulose is better suited for this application due to its chemical uniformity, easy functionalization, and superior flexibility and smoothness [40], [42].

Cellulose molecular structure consists of a chain of D-glucose units ($C_6H_{10}O_5$), where each unit is rotated 180° with respect the previous one. A unit bonds with the next through an oxygen atom between the carbon atom C-1 and the carbon atom C-4 of the next unit. Each unit has three reactive hydroxyl (-OH) groups connected to C-2, C-3, and C-6. The number of units forming the chain is referred to as the degree of polymerization. Units in the chain are locked in position because of the hydrogen bond between O3-H···O'5. This bond is present in all types of crystalline cellulose,

but bonds between O2 and O6 vary. These inter- and intra-molecular forces cause cellulose chains to aggregate, creating rigid crystalline structures. The strength of these bonds also explains why cellulose degrades before it melts – the hydrogen bond network is so extensive that cellulose chains cannot move freely, and cellulose undergoes thermal decomposition before enough heat can break this network [23].

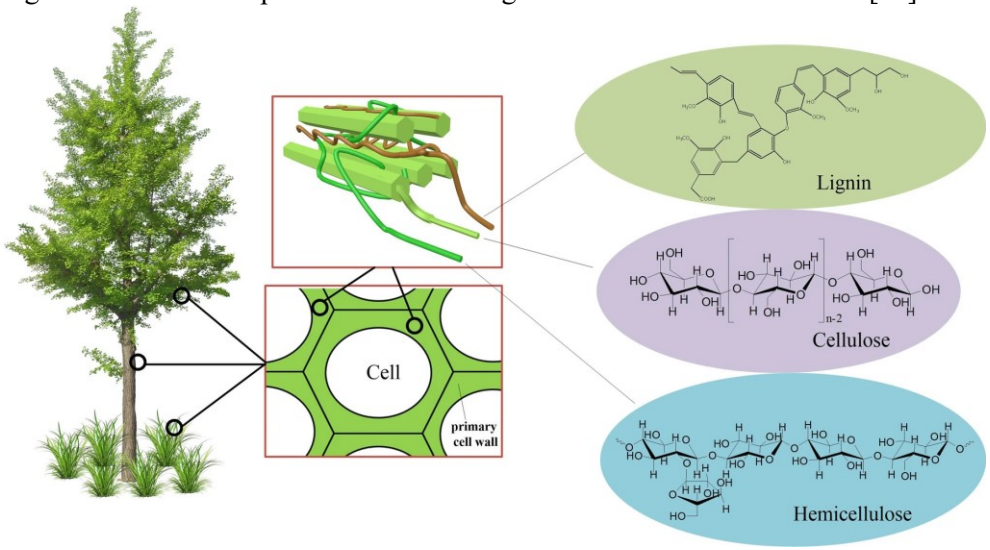

Figure 1. Cellulose, lignin, and hemicellulose in wood. Reproduced with permission under Creative Commons license [40]

Only a small number of solvents is able to directly dissolve cellulose; they are rather uncommon and often require strict operating conditions, such as ionic liquids and highly alkaline aqueous conditions [43]. To combine cellulose with simpler solvents, a simple strategy is the production of cellulose derivatives by replacing one or more of the -OH groups in the cellulose chains. The number of -OH groups replaced is known as its degree of substitution (DS), an average value ranging from 0 to 3, This parameter significantly influences the inter- and intra- molecular forces between cellulose chains and the solvent. In unmodified cellulose, these forces are responsible for cellulose's interaction with water, as it bonds with the -OH groups and gets trapped between fibers and amorphous regions, allowing cellulose to absorb large quantities without being dissolved [23]. Changing the functional groups will also impact the derivatives swelling, as they will have different levels of hydrophobicity than -OH groups.

The main strategy to process cellulose films is by dissolution and regeneration, that is, the removal of solvent. The resulting film properties are a result of the solution and its drying conditions [36], [44], [45]. Solution conditions include factors such as the functional groups, solvent type, concentration, DS, and the cellulose

chain length, known as the degree of polymerization (DP). The drying conditions include the casting surface, solvent volatility, ambient temperature, airflow, and relative humidity [46], [47]. It should be noted that unmodified cellulose and some of its cellulose derivatives are sometimes processed in water; unmodified cellulose is not soluble in water, and it is therefore a suspension, while other derivatives are truly soluble in water. As the films dry, the adopt the contour of the drying surface the cellulose chains start to arrange. The film optical and mechanical properties will depend on the chain and fiber arrangement.

Cellulose films have been considered as potential substrates for optoelectronics thanks to their sustainability relative to PET and PEN [18], [48]. There are two recent examples in the literature of successful use of cellulose films as substrates. The first one is an organic solar cell (OSC) with a 19% PCE built on ethyl cellulose (EC). One of the main issues when building a solar cell on cellulose is the film solvent resistance. As cellulose derivative films are made through dissolution and regeneration, these derivatives can interact and redisperse in the presence of different types of solvents. EC can be dissolved by chloroform, which is the main solvent of the ZnO nanoparticle suspension used to fabricate the first layer of the cell. To prevent damage to the substrate, the authors made a composite EC film with ethoxylated trimethylolpropane triacrylate (ETPTA). ETPTA is cured with UV light to polymerize it, forming a robust polymer network that prevents EC from redispersing in contact with chloroform. OSCs built on this substrate reached almost 19% efficiency [49]. The second example is the crosslinking of unmodified cellulose to form a so-called “vitrimers”, described as “dynamic covalently bonded cross-linked polymers, (that) merge the thermal stability of thermosets with the malleability of thermoplastics” [50]. Cellulose is first esterified with 10-undecenoyl chloride to replace some of the -OH functional groups, then it was made to react with (1,4-phenylenebis(1,3,2-dioxaborolane-2,4-diyl))dimethanethiol under UV light. This crosslinking is dynamic, meaning the cellulose network to break and reform, giving the film great plasticity while maintaining structural integrity. Thanks to this type of crosslinking, the cellulose vitrimer can resist water and other solvents, and with its high transparency and good mechanical properties it outperforms PEN as a substrate. Using this substrate, OSCs reached over 17% efficiency. These two examples show that using cellulose as a substrate for solar cells is indeed possible, with the right modifications. Cellulose films could be adapted to work with other types of optoelectronic devices, although this would require to customize cellulose to resist different types of solvents and withstand other deposition methods. These modifications are explored further in **Publication V**.

2.2 Perovskite solar cells

In the last 15 years, perovskite solar cells (PSCs) have attracted significant research interest. In 15 years, their efficiency has gone from 3.8% to over 25% [51]. Aside from their impressive efficiency, their fabrication is relatively easier than their silicon counterparts. Usually, PSCs are fabricated through solution-based methods, which lends itself to the use of different deposition techniques, such as spin coating, inkjet printing, slot-die coating, although perovskite evaporation has proven to yield very reproducible layers [52], [53]. Thanks to these fabrication routes and perovskite's low annealing temperature at around 100 °C, it is possible to use it in flexible devices with polymeric substrates like PET and PEN. Furthermore, PSCs are excellent candidates to be combined with silicon solar cells to form tandems that can achieve higher efficiencies by using a wider part of the solar spectrum [54]. In order to better understand how perovskites can be adapted to work with cellulose films, it is important to understand some basic concepts about them.

In photovoltaics, we usually mean organo-metallic halide perovskites when we say perovskite. It has an ABX_3 structure. A is a big atom or a small molecule, B is a metal like lead or tin, and X is a halide. The structure looks like metal B cations surrounded by six X anions, forming an octahedron. These octahedra form a crystal lattice, and the A cation sits in the interstices [55]. Perovskite can have different phases depending on the orientation of the octahedra, and this depends on the atomic radii of the components. What is the most stable phase in a perovskite can be calculated with Goldschmidt tolerance factor (t) (1):

$$t = \frac{r_A + r_X}{\sqrt{2}(r_B + r_X)} \tag{1}$$

where r_A, r_B, and r_X are the atomic radii of the A, B, and X, respectively [55].

Organo-metallic halide perovskites are photoactive in their cubic alpha phase, when their tolerance factor is close to 1. In the cubic alpha phase, the octahedra join through their vertexes, and are perpendicular to each other. When the tolerance factor is different from 1, the octahedra adjust by tilting, and this can cause the lattice to change to a different phase. This is mostly defined by the A and B atoms radii: if the A ion is too small or the B ion too large, the perovskite can take an orthorhombic or rhombohedral structure; or if the A ion is too big or the B ion too small, the structure can change to hexagonal or tetragonal [56]. Outside of the cubic alpha phase, the perovskite loses its photoactive property, which is something to be avoided. A perovskite might have a good tolerance factor, but the structure might become unstable overtime due to distortions [57]. These distortions can be a consequence of the degradation of the crystal due to the degradation of the organic component, or due to contact with water and oxygen, and lattice defects like atomic vacancies or ion migration inside the crystal during operation [58].

Perovskites' great advantage is their tunable bandgap, which can be adjusted across the ultraviolet to infrared spectrum by changing the constituent ions. This property makes them ideal to combine in tandem solar cells. Their bandgap comes from the hybridization of the *s* and *p* orbitals of the B and X ions, and this can be affected in many ways. As shown in **Figure 2a**, changing the X anion increases conduction band minimum (CBM) by increasing the Pb,*p* atomic level, due to the change in distance between B and X, leading to electron confinement that increases its energy. Meanwhile, the valence band maximum (VBM) shifts mostly due to the X anion electronegativity. In the case of the B cation, SnI compounds have lower electron affinity (EA) and ionization energy (IE) than PbI ones. EA is defined as the energy released when an electron attaches to an atom or molecule, and IE is the energy required to remove an electron from the valence band. As such, Sn compounds require less energy to move an electron from the valence band to the conduction band, effectively reducing the bandgap. Finally, while the A cation does not participate in the bonding that gives raise to the perovskite bandgap, it indirectly influences it by changing the lattice volume and introducing distortion in the structure. As the volume and lattice distortions increase, the BX octahedra tilt to accommodate to the structure, affecting how the *s* and *p* orbitals hybridize, ultimately changing the atomic levels [56]. In short, the conduction band is mainly defined by the B,*p* orbital, and the valence band is defined by the antibonding combination of the *s* and *p* orbitals of BX. In contrast, A has little influence in the electronic structure, but it plays a big role on the perovskite dimensionality, and thus, in its stability [59].

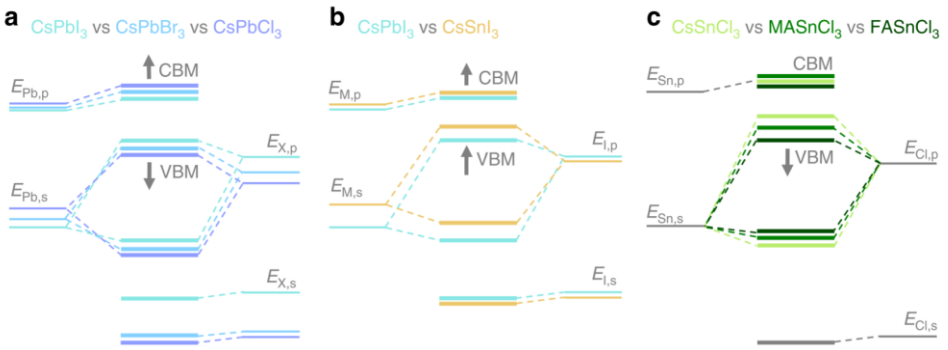

Figure 2. Energy levels in lead and tin perovskites. Reproduced with permission under Creative Commons Attribution 4.0 license [56]

These modifications provide a wide range of tuneable bandgaps suitable for PSCs (**Figure 3**). Additionally, the A cation and the X anion can be a mixture of different atoms or molecules. Methylammonium (MA) was the first organic

molecule used as the for the A cation site, but due to its tendency to degrade under light, moisture and oxygen more options have been explored. Perovskite made using formamidinium (FA) are more thermally stable than those using MA, yet, these perovskites are not thermodynamically stable at room temperature, undergoing a phase transition to a non-photoactive phase [60]. It was found that adding a large atom like cesium can help reduce trap states in the perovskite, and increase the device stability and performance. Nowadays, devices with the highest efficiencies are made with mixed A cations, mainly MA, FA, Cs, and Rb. Recently, guanidinium has been used as an A-site cation dopant, allowing for the fabrication of annealing-free PSCs with 19.25%. Normally, devices made without thermal annealing suffer from low efficiencies, as their annealing methods promote fast crystallization leading to the formation of small grains, thus, creating an abundance of charge recombination sites in the grain boundaries. The addition of guanidinium iodide facilitates the formation of an intermediate phase while the solvent is removed during annealing, leading to a better crystallization and higher efficiencies [61]. These results prove that further research is needed to optimize cation selection for perovskites.

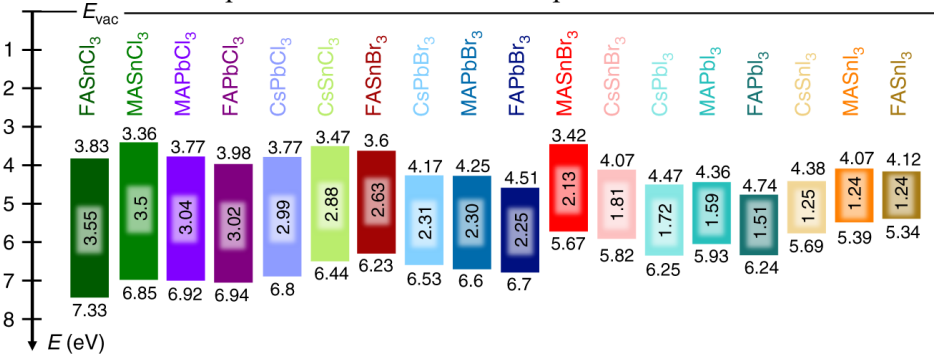

Figure 3. Different perovskite compositions with different bandgaps. Different perovskite compositions are arranged from left to right depending on their bandgaps in eV, from 350 to 1000 nm. The numbers over and under the bars correspond to the EA and the IE of each formulation, respectively. Reproduced with permission under Creative Commons Attribution 4.0 license [56]

Nevertheless, ion mixing comes its own set of problems, with phase segregation being one of the biggest. During the perovskite layer deposition and the PSC operation, regions rich on different A cations and X anions can form due to various factors. As it was explained above, the A-site cation strongly influences the perovskite crystal structure and stability, and its migration can lead to undesirable impacts. During film formation, when the antisolvent is being introduced, different phases form, and this is only exacerbated during thermal annealing. Because of perovskite's nature, activation energies for ion migration are low, allowing ions to migrate during operation, driven by difference forces. Ion migration is easily

activated under an electric field, and the effect is worsened at elevated temperatures (above 50 °C), leading to deterioration of the device [62]. This phenomenon is partially reversible when the device is left in the dark [59]. In the case of the X anion, bromide (Br^-) has a higher diffusivity in the solvent than iodide (I^-) due to its smaller ionic radius, and it tends to dominate the growth kinetics of the perovskite. PbBr-based compounds form easier than PbI-based ones, dominating crystal growth, ultimately leading to Br-rich regions. This dynamic indicates that the Br/I ratio is crucial to produce well distributed halides in the intended perovskite structure [63]. Additionally, in the perovskite lattice, halides are the ions with the lowest migration activation energy. Devices made with a Br-rich perovskite (except 100% Br) show high hysteresis, and show higher trap density. This is attributed to Br small size and easy migration through the crystal structure, leading to the formation to Br-rich phases [64]. These results show the sensitivity of this material– fabricating devices with perovskites can be challenging as it requires careful control of the crystallization process, which is affected by the surrounding atmosphere [65], light [66], deposition temperature [67], solvent evaporation [68], etc. One important factor that affects the perovskite crystallization is the surface morphology of the surface it is forming on, which greatly depends on its roughness [69]; this aspect will be explored later. First, it is necessary to discuss the design and fabrication of a PSC.

Designing a PSC starts with choosing a perovskite active layer material. Different applications require different perovskites because of the type of light and intensity that is available. To understand PSC operation, it is better to start with the active layer, and how the other layers relate to it. First, in the middle of the device, there is the perovskite-structure photoactive material from which the cell gains its name. When the perovskite absorbs light with energy higher than its bandgap, free charge carriers are generated. This process differs from organic solar cells, where a bound electron-hole pair (usually called exciton) is generated, and it needs to be separated by the other materials [55]. In perovskites, the excitonic binding energy is sufficiently low that the available thermal energy is enough to separate the charges immediately upon light absorption [55]. Perovskites are known for having large diffusion lengths, that is, free charge carriers can travel long distances before being reabsorbed by the bulk. The thickness of the active layer in a PSC is usually between 300 and 500 nm, which is enough for the charge carriers to reach the other layers. Next, the perovskite needs to have charge transport layers (CTLs) on each side to separate the charges. Introducing charge transport layers reduces the charge recombination rate, which increases the device performance [70], [71]. The CTL selection is mostly defined by the active layer bandgap and the relative energy levels of the conduction band (CB) and the valence band (VB), to ensure proper band alignment and efficient charge extraction, as well as fabrication considerations. Finally, electrodes complete the device and drive the charge carriers out to an

external circuit. Once the device is completed and it is illuminated, the active material should produce charge carriers that are extracted through the charge transport layers and the electrodes to an electrical load. The performance of the solar cell is then determined from its current-voltage (I-V) characteristics and key parameters derived from them [72].

While the plan to make a PSC starts with the active layer, its fabrication has to start on a viable substrate. Most PSCs are made on top of glass substrate covered with a transparent conductive oxide (TCO) that acts as an electrode. This material is normally deposited via sputtering and annealed at temperatures over 500 °C. ITO and FTO are the material of choice due to their high transparency, conductivity, and smooth surface [18]. This part of the cell is called the "bottom electrode". The bottom electrode needs to be thoroughly cleaned to allow for the proper deposition of the next layers, as defects can cause pinholes and material protrusions that can lead to low performance and even short-circuiting. Glass/TCO is typically cleaned with water and organic solvents in a sonication bath, followed by a plasma or ultraviolet-ozone treatment (UV-O_3). These treatments have two purposes: to eliminate all organic residues on the TCO surface, and to increase the bottom electrode wettability, as it greatly affects the spreadability of the next layer [73].

Next, one of the CTLs is deposited on the electrode. Which CTL is deposited first determines the solar cell structure; if the electron transport layer (ETL) is deposited first, the device is referred to as having a regular (or n-i-p) structure, otherwise it has an inverted (or p-i-n) structure [74]. It is worth mentioning that in the organic solar cell field the regular structure starts with the hole transport layer (HTL), to avoid confusion. One important factor to choose what CTL is deposited first are the material limitations. CTL materials that require high temperature annealing, like TiO_2 and NiO_x, need to be deposited before the perovskite, as it would destroy it [75]; some other CTLs need to be deposited after the perovskite due to solvent incompatibilities. From this point onward, the fabrication process is normally done in a nitrogen atmosphere to avoid water and oxygen intervening in the perovskite formation process. However, significant efforts are being made to improve the efficiency and stability of PSCs fabricated in ambient conditions [76].

Next comes the active layer, and it can be deposited either in one or two step process. In the one-step solution process (OSSP), the AX and BX_2 salts are mixed together in a solvent and deposited on the CTL-covered substrate, followed by antisolvent quenching to remove the solvent and start the perovskite crystallization. In the two-step solution process (TSSP), a solution of the BX_2 salt is deposited first, followed by the deposition of the AX solution. Both approaches have advantages and disadvantages: OSSP is overall easier to carry out and the films have a more defined stoichiometry, although optimizing the antisolvent quenching step is hard and can lead to an uneven deposition, while TSSP allows for more even deposition

and higher homogeneity at the expense of low stoichiometry control. Then, the substrate with the perovskite layer is typically thermally annealed at 100 °C to remove residual solvent and promote grain growth [77]. After the perovskite has cooled down, the next CTL is deposited. At this stage, the CTL deposition has to consider not damaging the perovskite with thermal treatments or solvents. Finally, the top electrode, typically gold, silver, or carbon is deposited, thus completing the device fabrication. **Figure 4** shows an envisioned PSC made on a transparent cellulose substrate, with a metallic nanowire bottom electrode, SnO2 as the ETL, a perovskite active layer, N^2,N^2,$N^{2'}$,$N^{2'}$,N^7,N^7,$N^{7'}$,$N^{7'}$-octakis(4-methoxyphenyl)-9,9′-spirobi[9H-fluorene]-2,2′,7,7′-tetramine (Spiro-OMeTAD) as the HTL, and a carbon top electrode.

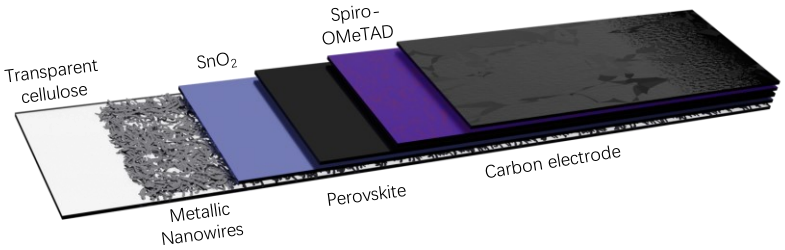

Figure 4. Envisioned PSC on transparent cellulose

For fabricating PSCs on glass substrates, the bottom electrode is typically pre-deposited by the supplier with an optimized surface roughness. Replacing glass with another material requires optimizing the deposition of the electrode (and the first CTL) on the new material to minimize negative effects on perovskite formation. Such a substrate replacement, in turn, requires understanding the substrate effect on the perovskite formation. Climent-Pascual et al. demonstrated that $MAPbI_3$:Cl perovskite prefers the 〈110〉 growth direction. The preferential (110) fraction increases with a reduce surface roughness, showing that the substrate not only has an influence on the interfacial properties of the perovskite, but also on the bulk properties [69].

Replacing glass for cellulose comes with many considerations: how is the electrode deposited on the new substrate? How do we optimize these layers to have

the best transparency with the lowest possible surface roughness and resistivity? How will these new materials impact the formation of the perovskite layer? If this new electrode forms a porous network, like metallic meshes and nanowires, how will solvents affect the substrates? The “traditional” deposition process of PSCs has been optimized to work on glass substrates over the years, and on PET and PEN to a lesser extent. Substituting glass and polymers requires reengineering all the methods involved into making a PSC. Cellulose films come with some limitations, yet most can be eliminated, or at least greatly reduced with the right modifications. Sustainable solar cells depend on finding the overlap between the restrictions posed by the properties of cellulose films and PSC fabrication methods.

3 Methods

3.1 Cellulose films fabrication and characterization

3.1.1 Cellulose casting

In **Publication II**, cellulose films were made to study how their processing affects their final properties. First, cellulose nanofibrils (CNF) were made from bleached birch pulp that was disintegrated with a high-pressure fluidizer (pressure of 1500 bar, Microfluidics M110P, Microfluidics Int. Co., Newton, MA) six times. CNF films were made by vacuum filtration from a CNF suspension in water, pressed between filter paper and steel plates and hot pressed. The optimal results were obtained using a 0.5% CNF concentration in water, 60 g/m^2, and pressing at 30 °C.

After optimization, nanocellulose of different grades was used to test the impact their functional groups on the final films. The same birch pulp was subjected to a TEMPO-mediated oxidation (2,2,6,6-tetramethylpiperidine-1-oxyl) process and passed through the microfluidizer once (TO-CNF). Other films were made using chlorine-free bleached softwood sulphite dissolving pulp and subjecting it to either an enzymatic (ENZ-CNF) or a carboxymethylation (CMC-CNF) treatment. ENZ-CNF was passed through the microfluidizer three times at 400 bar and five additional times at 1700 bar. CMC-CNF was passed only once through the microfluidizer at 1700 bar. Films made from these different nanocellulose grades were made in a similar fashion to the optimizer neat CNF ones.

In **Publication III** composite nanocellulose films were made using CNC, CNF, and montmorillonite clay (MTM). First, a 2 wt% CNC suspension in water sonicated and vacuum filtrated. A 2.18wt% CMC-CNF suspension was prepared in a similar fashion to that from **Publication II**. 25 g/m^2 CNC:CNF films were cast on polystyrene Petri dishes and dried overnight at 23 °C and 50% relative humidity. CNC:CNF films were made with 100:0, 75:25, 50:50, 25:75, and 0:100 mass ratios. The films containing MTM consisted of 50:50 cellulose (CNC: CNF): MTM by mass. All the films made in **Publications II and III** were prepared by our collaborators.

3.1.2 Angle dependent transmittance

In angle dependent transmittance, the sample is mounted on an aperture of an integrating sphere; inside this sphere there is a highly reflective polymer that directs all the light to an optic fiber cable to takes it to a spectrometer. This solution also allows rotation of the integrating sphere and the sample, enabling measurement of how the transmittance is affected by the light incidence angle. Our setup consisted of an Artifex Engineering 100 mm integrating sphere coupled to a motorized rotating stage. A Thorlabs SLS201L/M Stabilized Tungsten-Halogen Light Source was used as a white light source, coupled to a Thorlabs SLS201C collimator and a pair of lenses. The light from the integrated sphere is transmitted through an optic fiber to a Thorlabs CCS200/M compact Czerny-Turner spectrometer (**Figure 5**). This technique was used to analyze the cellulose films made for **Publications II and III**. The data obtained is weighted against a 1.5 AM solar spectrum to simulate the transparency they would have under a solar simulator.

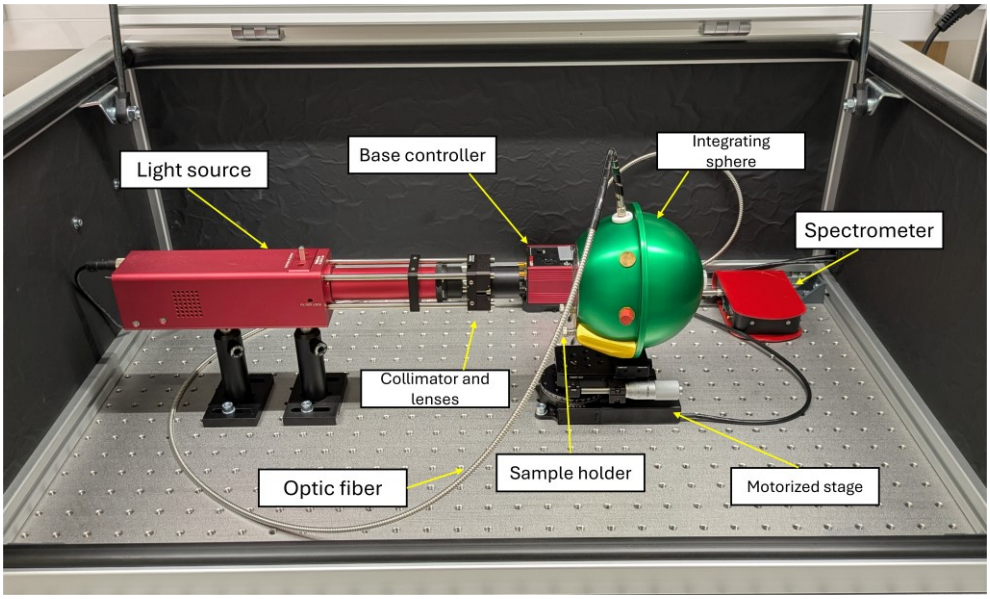

Figure 5. Angle dependent transmittance setup at the University of Turku.

3.1.3 Tensile testing

To measure the mechanical properties of the films made for **Publication II and III** the films had to be preconditioned by maintaining the films in a controlled environment with 50% relative humidity at 23 °C for several days. The films are then cut in strips 30 to 45 mm long and 6 mm wide and subjected to a tensile test using an MTS 3125 tensile tester to obtain their stress-strain curves at a strain rate

of 5 mm/min. These tests were done by our collaborators at RISE Research Institutes of Sweden.

3.1.4 Atomic force microscopy

Atomic force microscopy (AFM) is a microscopy technique used to image the surface of samples in the nanometer scale thanks to its ease-of-operation and high resolution compared to SEM. Unlike optical and electron microscopies, AFM generates the images by dragging a very fine tip over the sample surface to measure its topography and other properties. It has some advantage over SEM and TEM systems: it can produce high quality surface images at a fraction of the cost, it is simple to operate, and it does not need special measurements conditions like high vacuum or low temperatures; however, it does take significantly longer to get good quality measurements.

AFM works by using a very fine tip mounted on a silicon cantilever to scan a surface. Light reflected from the cantilever is measured by a photodiode, ultimately transforming the cantilever movements into electrical signals. These signals are recorded for each pixel of the measured area, creating the image. The tip is also connected to piezoelectric transducers that measure the force applied to the tip to know how close it is to the sample surface. These components are connected to PID controllers to regulate the movements of the instrument.

To measure the topography of a surface, AFM can be divided in in two modes: contact and oscillating. In contact mode, the cantilever deflection is a direct result of the topography of the sample, without the need of a lot of processing that can slow down imaging, making it a relatively fast method. When the cantilever is close to the sample surface, it experiences a repulsion force; the AFM system tries to keep the cantilever repulsion at a constant value (known as the set-point) to avoid tip deflection and minimize errors. In oscillating mode, as its name implies, the tip is oscillating at a constant frequency and the amplitude and frequency changes due to the interaction between the tip and the sample surface. Oscillating mode can be further divided in non-contact mode, where the tip oscillates close to the sample surface and experiences only attractive forces, and tapping (or intermittent) mode, where the tip moves through the repulsive and attractive regimes. Tapping mode use is favored in air, while non-contact mode is used in vacuum conditions. Nonetheless, non-contact mode can produce as good results, and often better, as tapping mode due to lower tip wear [78].

In **Publication III**, a ParkSystems NX10 AFM microscope in non-contact mode was used to gather surface morphology images from cellulose samples. The images were further processed using Gwyddion to obtain statistical data and 3D images of the sample surface.

3.2 PSC fabrication and characterization

3.2.1 Spray coating

In spray coating, a liquid solution is atomized by a carrier gas to evenly distribute it over a surface. This method is low-cost and easy to upscale due to its simplicity, being one of the few that can be used both in a laboratory scale as well as in industry. An airbrush similar to the one in **Figure 6** was used to spray coat some materials to make PSCs. To operate it, a gas needs to be pumped through the gas inlet, typically compressed air or pressurized nitrogen; the gas is released when pressing and pulling the trigger, making the gas pass below the solution chamber, carrying the solution through the nozzle and onto the substrate. The deposited film morphology can be controlled by controlling the spray rate, the gas pressure, and the amount of solution used [79]. While devices made through spray coating with airbrushes can achieve high efficiencies, the method is difficult to optimize and requires a skilled operator [79].

Figure 6. Airbursh cross-section. Reproduced with permission of Wiley [79]

In **Publication IV**, for PSCs made on glass/FTO, spray pyrolysis is used to deposit a layer of crystalline titania (c-TiO_2) to act as the ETL. First, a 25 ml solution was made with 2 ml diisopropoxytitanium bis (acetylacetonate), 1 ml of acetylacetone, and 22 ml of ethanol. This solution is evenly sprayed over clean glass/FTO substrates held at 460 °C to form a c-TiO_2 layer of around 40 nm thickness.

3.2.2 Spin coating

Spin coating uses centrifugal force to spread a liquid evenly over the surface of a rotating substrate, at speeds between 1000 and 10 000 rpm. This technique can make coating as thin as a few nanometers, making it particularly useful for thin film fabrication. Because the solvent evaporation can be greatly increased by airflow caused by the high spinning speeds, the coating and drying of the substrate can be done in the same step. Spin coating is a widespread PSC fabrication method thanks to its simplicity, low-cost, and relatively even deposition [80]. Although, only one device can be processed at a time, it is seen mostly as a method for trying and testing new formulations before production upscaling. Spin coaters are simple machines, mainly consisting of a place where the substrate can sit still while rotating, known as the chuck, and it is maintained in place with a vacuum force. Around this setup there are walls that catch the residues ejected during rotation. The spin coater electronics help set up coating programs by controlling the coating speed, acceleration, time, and number of steps. The coating solution can be spread over the substrate before the spinning program, or during spinning, known as "dynamic spin coating".

In **Publication IV**, part of the ETL, the active layer, and the HTL were spin coated to make PSCs. Around 50 µl of a 150 mg/ml suspension of 30-NRD TiO_2 paste in ethanol were spin coated on c-TiO_2 covered substrates, followed by another annealing step at 450 °C for 30 minutes to complete the mesoporous titania layer (m-TiO_2). After the films have cooled to room temperature, they are subjected to a UV-O_3 treatment for 15 minutes, then transferred to a nitrogen-filled glovebox for spin coating with the perovskite active layer. The perovskite precursor solution is a mix of three solutions in different proportions to make a $Cs_{0.05}(FA_{0.83}MA_{0.17})_{0.95}Pb(I_{0.83}Br_{0.17})_3$ (CsFAMA). First, a solvent solution is prepared using a 4:1 V/V proportion of dimethylformamide (DMF) and dimethyl sulfoxide (DMSO). This solvent is used to prepare 1.5 mol solutions of PbI_2 and $PbBr_2$; another CsI 1.5 mol solution is prepared with only DMSO. The PbI_2 and $PbBr_2$ solutions are mixed with FAI and MABr, respectively, with a stoichiometry of 1:1.09 (9% lead excess). These two solutions are mixed in 5:1 V/V ration, then complemented with 5 vol% of CsI in DMSO to obtain a $Cs_{0.05}(FA_{0.83}MA_{0.17})_{0.95}Pb(I_{0.83}Br_{0.17})_3$ (CsFAMA) perovskite precursor. The precursor solution is cast on the TiO_2-covered substrate and spun at 1000 rpm for 10 s for even spread, then at 6000 rpm for 20 s. 10 s before the end of the program, 200 µl of CB are dynamically spin coated on the substrate to quench the perovskite layer and remove the solvent. The sample is then thermally annealed at 100 °C for 1 h.

The HTL is made with a 70 mM Spiro-OMeTAD solution in CB, doped with 4-*tert*-butylpyridine (tBP), lithium bis(trifluoromethanesulphonyl)imide (LiTFSI, Sigma Aldrich) and tris(2-(1H-pyrazol−1-yl)−4-*tert*-butylpyridine) cobalt (III) tris-

(bis(tri-fluoromethane) sulphonimide) (FK209). After returning to room temperature, the substrates are dynamically spin coated with the Spiro-OMeTAD solution at 4000 rpm for 10 s. The substrates are then left inside a dry box overnight to allow oxidation of the Spiro-OMeTAD (HTL), which increases its conductivity.

3.2.3 Thermal evaporation

Metal top electrodes for PSCs are typically thermally evaporated, and usually made of gold or silver. This is done inside a chamber with ultra-high vacuum (pressures below 1.5 x 10^{-5} mbar), where the metal is heated to be vaporized. Vaporization can happen in molten metals (i.e., Al and Sn) or solids (i.e., Cr and Mg) [81]. The vaporized metal then condenses on the substrate surface, forming a thin layer that serves as an electrode. In **Publication IV**, gold was thermally evaporated to form an 80 nm thick electrode on top of the HTL to complete the solar cells.

3.2.4 3D printing of characterization holders

In **Publication IV**, holders were made through 3D printing to characterize PSCs and investigate if there are differences between devices made on etched and unetched devices. This distinction is important for solar cells made on cellulose, as some types of electrodes (i.e., metallic nanowires) cannot be etched if embedded inside the cellulose matrix, and etching chemicals and laser could damage the substrate. The holders were made from EasyABS filament in a Prusa MK3S+ 3D printer with a 0.4 mm stainless steel plate. Harwin P70-1020045R spring-loaded “pogo pins” were inserted and glued to the 3D printed holder and soldered to copper wires. Neodymium magnets were added to each corner to fix the cell in place. The cells are accompanied by a brass characterization mask with a defined aperture area. This holder was designed to have constant contact between the pin and the electrode at different points of the cells without using alligator clamps that could damage PSCs made on cellulose (**Figure 7**).

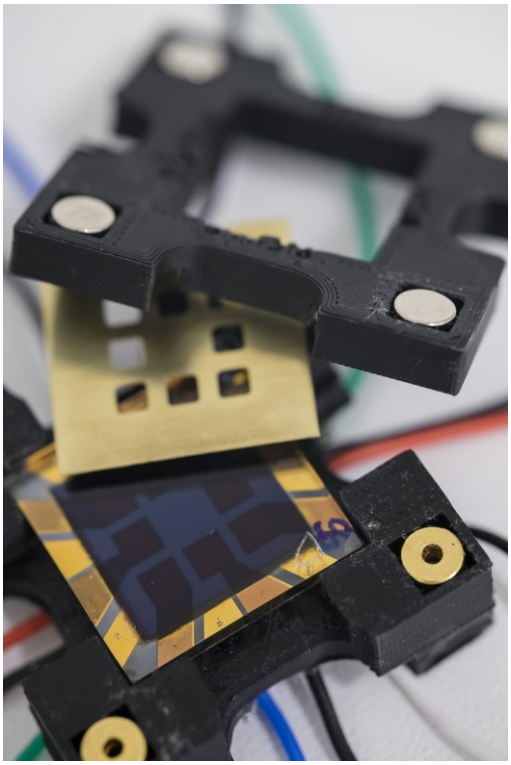

Figure 7. 3D printed holder with an 8-pixel PSC and characterization brass mask. Reproduced with permission under Creative Commons Attribution License 4.0 [82]

3.2.5 Current-voltage (IV) characterization

The four key parameters used to evaluate the performance of a solar cell are: open-circuit voltage (V_{OC}), short-circuit current (I_{SC}), fill factor (*FF*), and its *PCE*. Under open-circuit conditions, meaning that the cell is illuminated and not connected to an external load, the generated electrons move to the ETL and the holes to the HTL, accumulating at the interfaces. This charge separation creates a charge difference between the electrodes, which is the voltage generated in the cell. It can be deduced from the difference in energy levels between the ETL and the HTL, and it is affected by the quality of the perovskite layer and charge recombination. In a sense, V_{OC} is the voltage generated in the cell when illuminated and connected to a load with infinite resistance. In a similar manner, connecting the illuminated cell to a load with zero resistance gives I_{SC}. This parameter is a measure of how many charge carriers can be extracted from the cell; the more light with higher energy than the perovskite bandgap reaches the active layer, the more charge carriers are generated. I_{SC} is greatly affected by the resistivity of the materials and interfaces, by carrier recombination due to trap states, and by temperature. Usually, the short circuit

current density (J_{SC}), is reported instead, as it allows for a better comparison between devices by considering the cell active area.

FF measures the performance of a solar cell (2). *FF* represents the "squareness" of the JV curve; it is the relation between power generated at the maximum and the power that would be generated at ideal conditions [72], defined as:

$$FF = \frac{V_{max} \times J_{max}}{V_{OC} \times J_{SC}} \quad (2)$$

The efficiency of the cell (*PCE* or η) is defined by the relation of how much power is being generated and the power of the light shone on the cell (3):

$$PCE = \frac{J_{SC} \times V_{OC} \times FF}{P_S} \quad (3)$$

where P_S is 1 sun, equal to 1000 W/m^2. All these values are illustrated in an IV curve (or JV is using the current density) (**Figure 8**).

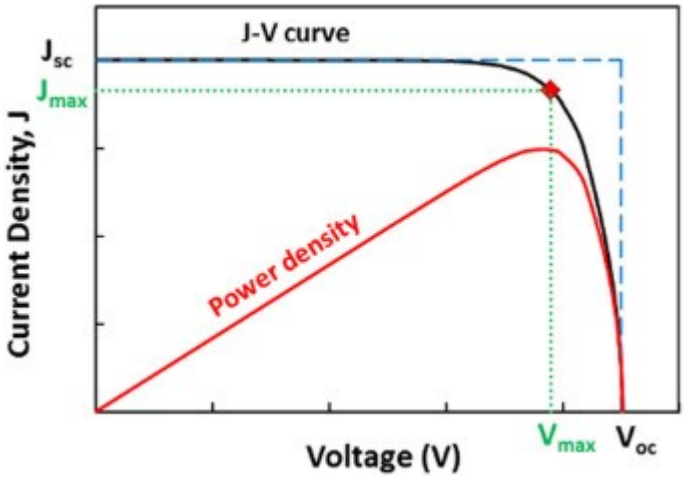

Figure 8. Power density (red) and current density (black) as a function of voltage. Reproduced with permission of Elsevier [72]

In **Publication IV** the 4-pixel cells were characterized using a Newport Oriel Instruments model 92 250A solar simulator at 1 sun illumination, and a Keithley 2636 source measure unit (SMU). The cells were covered with a brass mask with a 12 mm^2 aperture to only measure the power produced by a known illuminated area. The 8-pixel cells made by our collaborators were characterized using a Wavelab Sinus-70 solar simulator and a Keithley 2450 SMU using a brass mask with a 10 mm^2 aperture. Both groups were characterized with a 50 mV/s scan rate.

3.2.6 Electrochemical impedance spectroscopy

Electrochemical impedance spectroscopy (EIS) is a technique to characterize the electrical and electrochemical properties of PSCs during operation by measuring the impedance response to small electrical signals of varying frequencies. One advantage of PSCs is that they require low energies to form; however, this also means they can be easily affected in many ways. Inside a PSC there are a multitude processes occurring at the same time: degradation from moisture, oxygen, and UV light, ion migration due to electrical fields created inside the device during operation, and radiative and non-radiative carrier recombination [83]. All of these processes have different timeframes, as illustrated in **Figure 9**.

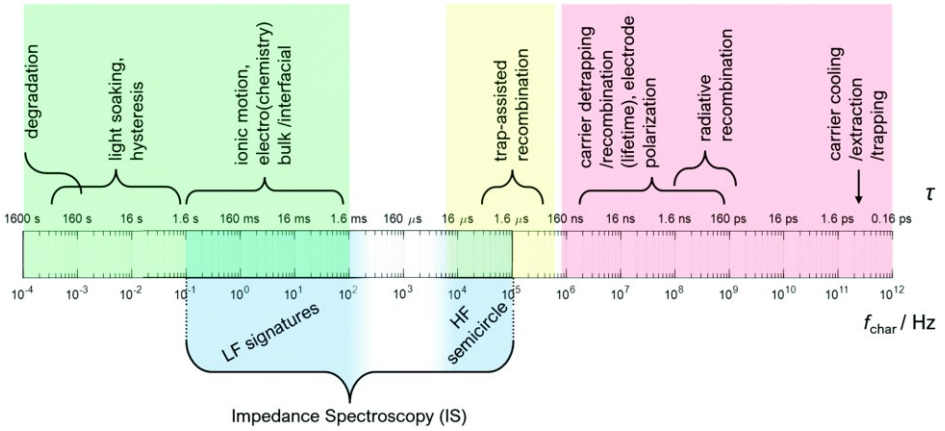

Figure 9. Dynamics in a PSC. Reproduced with permission under Creative Commons Attribution NonCommercial 3.0 Unported License [83]

By introducing a small electrical sine wave signal of a known frequency and measuring the impedance change in the device, it is possible to know how long it takes the device to return to an equilibrium state. This information is compared to an equivalent electrical circuit (EC) (**Figure 10a**) that would show a similar behavior, allowing for a better understanding of the underlying physics of the device. As shown in **Figure 9**, IS can only provide information about certain processes, because the timeframe of other phenomena is either too slow, like device degradation, or too short, like radiative recombination. Therefore, EIS is mostly useful to measure ionic migration and trap-assisted recombination. EIS is often carried out as a complement to IV characterization, and it can give useful information to understand the reasons behind a cell performance.

EIS information is laid out in a Nyquist plot, where the impedance real component is on the X-axis, and the imaginary component is on the Y-axis. PSC EIS measurements typically appear as semicircles (**Figure 10b**), with the high frequency

measurements on the left side of the graph and the low frequency ones on the right; these semicircles can be compared to the electrical response of a resistor-constant phase element (R-CPE) circuit (**Figure 10a**). The first element, the series resistance (R_S), is derived from the distance between the origin and the start of the semicircle. R_S is a purely resistive value; thus, it only has an X component, and it is the ohmic resistance between the cell electrodes. The first semicircle corresponds to the high frequency responses inside the cell, such as the non- radiative recombination processes, and it is represented in the EC by a CPE and a resistor in parallel. The resistor corresponds to the semicircle diameter on the X axis, and the CPE is responsible for the "flatness" of the semicircle. The second semicircle thus corresponds to the low frequency response attributed to ion migration inside the PSC. This information complements the IV results giving information about how charge transport affects the cell performance. R_S highly impacts the cell *FF*, ultimately lowering *PCE*. A low R_{Rec} signals high charge recombination happening in the cell, lowering the cell V_{OC} and I_{SC}. At the furthest to the right R_{Ion} indicates the resistance of mobile ions to move inside the perovskite layer and across the interfaces. A low R_{Ion} indicates that ions move too easily and this causes undesirable hysteresis. Ideally, a solar cell should have low R_S, but high R_{Rec} and R_{Ion}.

EIS was performed on the cells made in **Publication IV**, using a Gamry Reference 600+potentiostat from 10^{-1} to 10^{6} Hz and a Peccell PEC-L01 solar simulator.

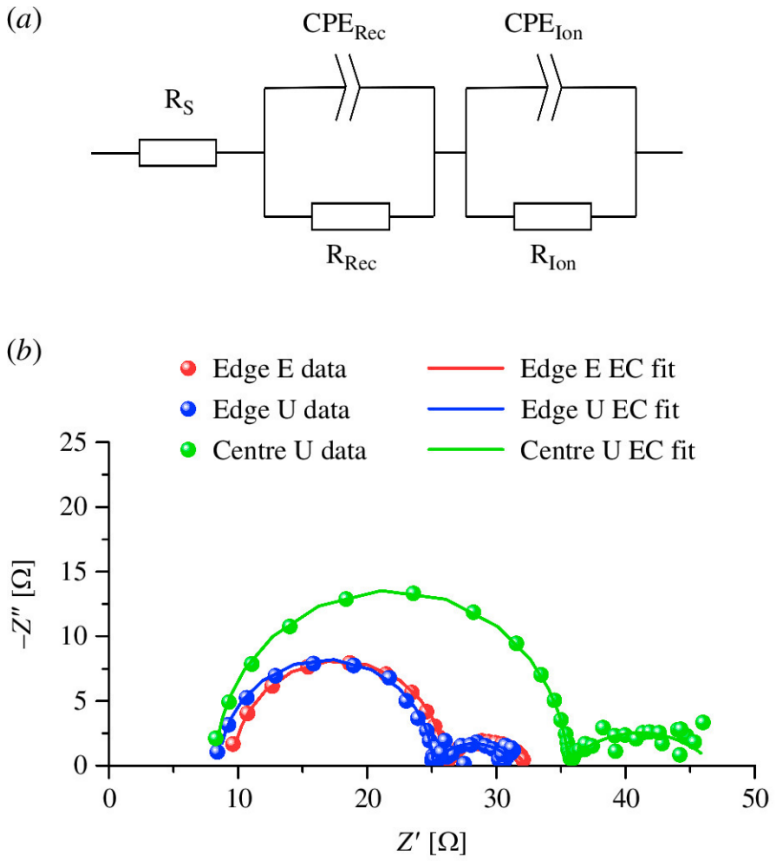

Figure 10. (a) EIS equivalent circuit; (b) EIS of PSCs measured at different points on the electrode surface. Reproduced with permission under Creative Commons Attribution License 4.0 [82]

4 Results and discussion

4.1 Impact of cellulose processing and drying on film properties (Publications I, II, and III)

4.1.1 Bio-based materials for solar cells

A set of bio-based materials were reviewed in **Publication I** to evaluate their potential as greener alternatives to valuable or scarce materials in photovoltaic devices (**Figure 11**). One of the best examples is transparent wood as a substrate; after removing lignin and replacing it with a transparent epoxy resin with a matching refractive index, a PSC with 16.8% was built [84]. The low efficiency, compared to the state-of-the-art, is partly due to the substrate thickness, reducing the amount of light that reaches the active layer. Cellulose films, on the other hand, have the advantage of being very thin and highly transparent, as they are made of pure cellulose and do not need to go through lignin removal and resin incorporation steps.

Cellulose films offer easy processing, flexibility, and high transparency in contrast with transparent wood; however, cellulose films tend to have high surface roughness and can be affected by solution-based fabrication methods. The surface roughness depends on the fiber size being used and the fabrication method, while solvent interactions highly depend on the cellulose functional groups and the number of available -OH groups. One way to reduce the surface roughness is using nanosized cellulose materials to make films, but it only reduces it to a few micrometers – still three orders of magnitude higher than glass. CNC can reach roughness levels of a few nanometers, but CNC films are too brittle and break easily. On the other hand, during fabrication it is desirable that cellulose films can be made using common solvents, however, this becomes a problem when depositing material using a solvent that can redisperse cellulose. In **Publication I**, it was proposed to use a planarization layer to reduce the surface roughness, protect the film from solvents, and increase the gas barrier levels. It has to be stated that the selection of this layer needs to be carefully selected, and its environmental impact should not be understated – while the substrate is bio-based, it risks "greenwashing" the substrate-coating array.

Figure 11. Possible bio-based components in solar cells. Reproduced with permission under Creative Commons Attribution License [85]

One of the main objectives of **Publication I** is to challenge greenwashing; including biobased materials does not automatically make something greener. The viability of the product that uses biobased materials should be judged based on economic and environmental criteria, i.e. their return on energy investment (REI). The REI analysis considers the energy produced by the device during its lifetime versus the energy invested to fabricate it, giving rise to three categories of biobased materials: those that are near to be implemented, promising ones that need further research, and materials with low performance meant for specialized applications. In this analysis, cellulose films fall in the second category, as it shows great promise, but many properties need to be improved, such as their gas barrier properties and their surface morphology without sacrificing their mechanical and optical properties.

4.1.2 Processing factors affecting roughness, optical and mechanical properties of nanocellulose films for optoelectronics

In **Publication II** results are divided in two parts: the first is on how the film properties can be changed using a single type of CNF, and the second is on different types of CNF with the optimized parameters from the first section. One of the first things observed that have an impact on the film formation was the cellulose suspension stability and homogeneity. Low concentrations (0.1 wt% in water) led to

phase separation after 24h, due to the poor network stabilization and less interaction between the nanofibrils. After casting the films, it was observed that those made with high concentrations (1.5 wt%) had higher opacity, reflectance, and haze at 550 nm, caused by CNF flocculating in suspension, before the film formation. It was also observed that higher concentrations led to an increase in surface roughness due to the formation of agglomerates, which would be unfavorable when fabricating PSCs. Films made with a 0.5 wt% presented the lowest surface roughness (500 nm) and very high transmittance (~86% at 550 nm), therefore, this concentration was chosen for the second section.

Increasing the films' grammage and the pressing temperature both decreased the optical transparency, but for different reasons. Pressing at 90 °C results in quicker water elimination, disrupting the formation of hydrogen bonds between cellulose chains, leading to a reduction in shape. Film density increased with the grammage, elongating the path light has to travel across it, ultimately reducing the transmittance (**Table 2**). It was also observed that as density increases, so do the reflectance and haziness, and observing the difference in surface roughness, there is no clear correlation. This effect indicates that optical properties are affected more by the internal structure of the film than its surface. Mechanically, changes on the parameters discussed above have a noticeable effect on the films' tensile strength. An increase in density meant higher fiber compaction, which require more energy to break. Also, films made with low concentrations and pressed at low temperatures presented better mechanical properties, probably due to the random orientation of the fibers.

Table 2. Properties of various films made with difference NC grades. Reproduced from Publication II

NC	Conc (wt%)	Gramm. (g/m²)	Temp. (°C)	Thickness (µm)	Density (g/cm³)	Tensile strength (MPa)	Roughness bottom side (µm)	Roughness top side (µm)	T (%)	R (%)	H (%)
CNF	0.1	30	30	23 ± 1.0	1.12 ± 0.03	237 ± 5	1.5 ± 0.2	1.3 ± 0.2	86	12	55.5
CNF	0.5			26 ± 3	1.07 ± 0.02	192 ± 11	0.5 ± 0.1	0.6 ± 0.1	86	11	50.7
CNF	1.5			33 ± 5	1.05 ± 0.05	153 ± 15	0.7 ± 0.04	1.0 ± 0.2	85	10.5	50.7
CNF			90	18 ± 1	1.25 ± 0.02	233 ± 5	0.3 ± 0.04	0.5 ± 0.04	82	17.8	55.1
CNF	0.5	60	30	47 ± 2	1.11 ± 0.02	196 ± 5	1.5 ± 0.1	2.0 ± 0.2	84	12.5	50.4
ENZ-CNF				43 ± 2	1.09 ± 0.10	133 ± 4	1.4 ± 0.2	1.0 ± 0.1	83	14.4	71.9
CMC-CNF				54 ± 1	0.95 ± 0.02	173 ± 8	2.7 ± 0.7	1.0 ± 0.1	86	10.9	66.7
TOCNF				**47 ± 2**	**1.3 ± 0.05**	**188 ± 6**	**1.2 ± 0.2**	**0.8 ± 0.1**	**86**	**10.7**	**50.4**

In the second section of the article, films of different grades of CNF were made to study the effects of different functional groups and treatments. The same CNF used for the first batch of films was subjected to TEMPO-oxidation treatment, in which –OH groups were converted into carboxyl (–COOH) groups. Then, CNF from another supplier was subjected to a carboxymethylation treatment to bond the -OH functional groups with chloroacetic acid following Wågberg et al. protocol [86]. The same CNF was also subjected to an enzymatic treatment. Regular CNF and the enzymatic CNF (CNF and Enz-CNF) kept the -OH functional groups, whereas the TEMPO-oxidized and the carboxymethylated CNF (TOCNF and CMC-CNF) have different functional groups.

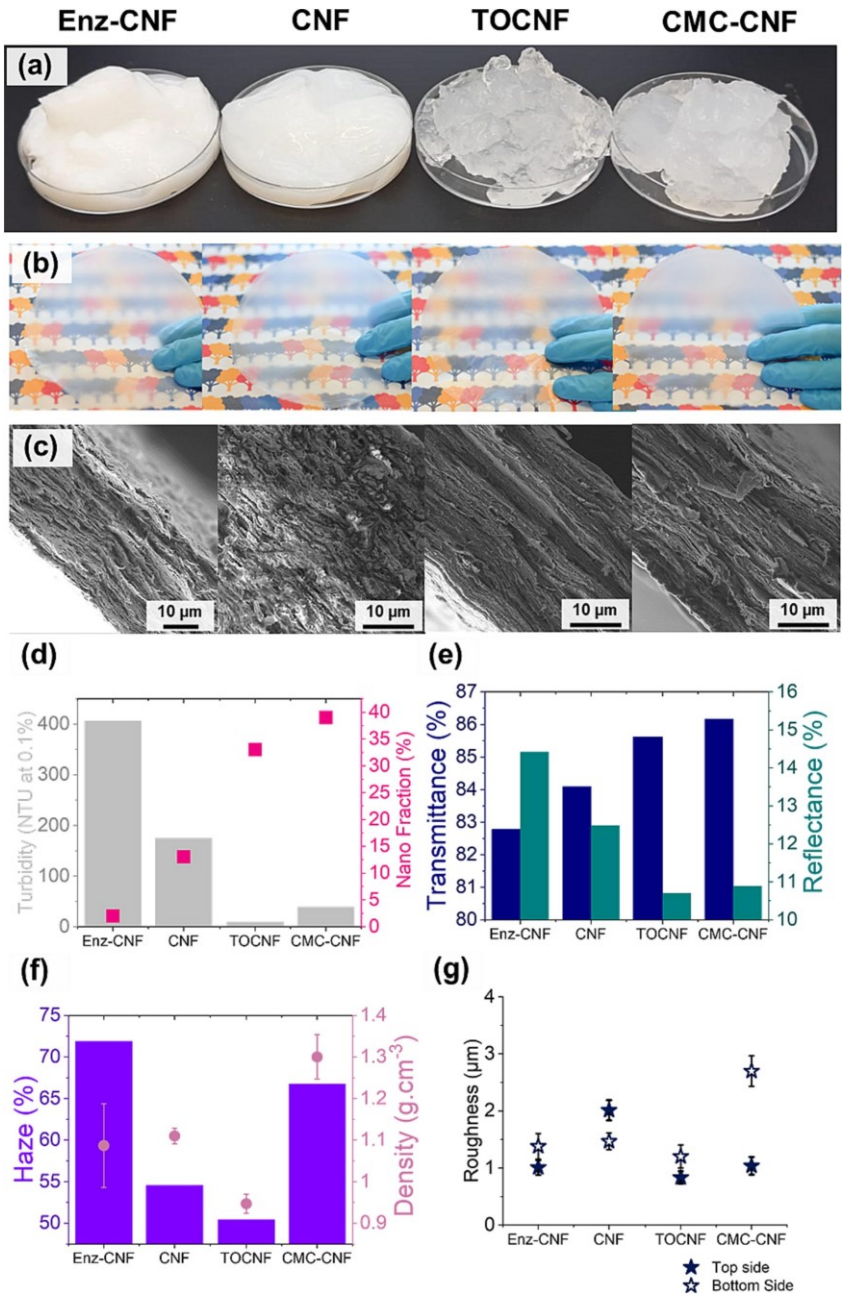

Figure 12. Different CNF grades and their properties. (a) CNF source pulp. (b) Films made with different CNF grades. (c) SEM cross-section images of CNF films. (d) Suspensions turbidity and nanofriction. (e) Transmittance and reflectance at 550 nm. (f) Haze at 550 nm and grammage. (g) Roughness on both sides of the films. Reproduced with permission under Creative Commons license CC-BY [36]

It was initially hypothesized that the suspension turbidity could indicate what the optical properties of the film would be, but in the case of Enz-CNF its lower transmittance and higher reflectance can be attributed to voids in the films created by the longer fibrils that increase the light scattering. The cross-section SEM pictures (**Figure 12a**) show that all films have laminar structures, yet TOCNF and CMC-CNF have different densities due to the interaction of their functional groups with water. Water removal in CMC-CNF films was slower, leading to denser films. Furthermore, since these films were produced through vacuum filtration, the side that is in contact with the filter tends to have the higher surface roughness, as the large fibrils tend to settle at the bottom. But even the "smoothest" film still had a surface roughness over 1µm, which is quite high compared glass at around 1 nm.

Normally, denser films lead to better mechanical properties, but this is only true when comparing the same CNF grade. CNF films were stronger than Enz-CNF because the fibril size homogeneity led to better compaction and better interaction, requiring more energy to break. In the case of Enz-CNF and CMC-CNF, carboxyl groups induced higher fibrillation leading to enhanced assembly and entanglement. Since regular CNF and TOCNF films were made from the same base CNF, it was expected that the carboxyl groups would have the same effect, yet TOCNF films had lower mechanical properties as they were too fibrillated.

Optical transmittance is one of the most important properties for a solar cell substrate. Transmittance is usually measured with a UV-Vis spectrometer where light is shone on a semitransparent sample and measured on the other side to know what is its transparency to different wavelengths. The limitation of this approach is that it can only measure light that passes directly through the material and is not refracted away from the detector. This problem can be solved by trapping all the light scattered by the sample inside a very reflective body (i.e., an integrating sphere) and sending it to a spectrometer. This approach can be complimented with a motorized base to rotate the integrating sphere, resulting in transmittance measurements that are now angle dependent. Measurements like this are important as it has been proven that cellulose can work as an antireflective coating [87], [88]. In the last section of the article the films were analyzed through angle dependent transmittance, to see how well these films would perform as substrates for optoelectronics. While highly transparent when light is perpendicular, the films exhibit high light scattering, reflecting light as the angle increases, dropping from >90% at 0° to 60% at 65°. Compared to glass, PET, and PEN, CNF films are highly reflective at different angles, which can lead to less light entering the active area of a solar cell. Fang et al. [89] used a cellulose film as an antireflective coating on a solar cell to increase its photocurrent by scattering light increasing its pathlength across the cell, giving light a higher chance to be converted into electricity. This approach can lightly increase the cell efficiency, yet it can only work when the

antireflective coating refractive index is carefully tuned, requiring a good control of the film thickness and porosity [90].

4.1.3 Multifunctional nanocellulose hybrid films: From packaging to photovoltaics

In **Publication III**, CNC and CMC-CNF were combined to make composite films. CNC films are generally brittle, and the addition of CNF can help increase the film flexibility, thanks to the long fibrils. MTM clay was also added to some of the films in an attempt to decrease the films gas permeation. Films made of CNC and MTM were denser, as the their small size allows for better packing, reducing voids in the structure, meanwhile, adding CNF decreases the density as it interrupts the CNC:MTM layered structure.

Mechanically, CNC and CNC:MTM films have no significant differences, since their small size and limited entanglement limit the tensile strength. Other than in the 75CNC:25CNF film, the addition of MTM decreases the film strength as clay interrupts the nanocellulose network. Comparing the films in this study with those from other publications [91], [92], [93], hybrid films made of CNC:CNF show worse mechanical properties than those made with CNF:MTM mixtures, indicating that CNC has a bigger impact than MTM. Regarding the water interactions, cellulosic materials tend to do poorly at blocking water because of their hydrophilic nature. Films made entirely of CNC completely redispersed in water, but managed to resist, even with a low swelling percentage, thanks to their intercalated "brick and mortar" structure. For CNC:CNF:MTM films, MTM had an overall positive effect lowering the films swelling.

MTM was added to help reduce the films' water vapor transmission rate (WVTR), as the MTM forms a brick-and-mortar structure between the cellulose layers, slowing down water vapor going through the film. In mixed CNC:CNF films there was a small decrease in WVTR from 144.2 to 133.1 $g/m^2 \cdot day$, but MTM had the opposite effect in pure CNF films. Unfortunately, their water vapor transmission rates (WVTR) values are still too high compared to the 10^{-3} to 10^{-6} $g/m^2 \cdot day$ level required for optoelectronic substrates [94].

Optically, CNC:CNF films have transmittance levels over 80% at 550 nm without much variation. Neat CNC films form chiral nematic structures, giving CNC films an iridescent appearance. While transparency remains high, films containing CNF are hazy due to air voids between the fibrils, scattering light. The main optical impact of adding MTM was the blocking of UV light below 300 nm but at the expense of lowering the overall transmittance across the visible part of the spectrum. Because of MTM tendency to decrease transparency, and its reduction in water

uptake and WVTR are not significant, it was decided to focus on purely cellulosic films.

Similar to **Publication II**, angle dependent transmittance was done to characterize the CNC:CNF films to judge their possible application in optoelectronics. The transmittance of all films containing CNF drops as the light incidence angle increases, due to light scattering produced by voids in the cellulosic structure. Neat CNC films show an increased reflection of wavelengths between 500 and 700 nm due to the chiral nematic formation of the nanocrystals (**Figure 13**). This reflection can be shifted by ultrasonicating the CNC suspension before casting to further break the nanocrystals, moving the reflections to the infrared part of the spectrum [95].

The CNC:CNF films surface morphology was analyzed using AFM. Measurements showed that neat CNC had the lowest surface roughness at 17 nm, while the neat CNF had the highest at 229 nm; the other films being somewhere in between. This is due to CNC more compact size, forming denser films, instead of porous structures like CNF. Still, the smoothest film is 4 times rougher than PET and PEN. Considering the brittleness of pure CNC films, this set of films is unsuitable for optoelectronics.

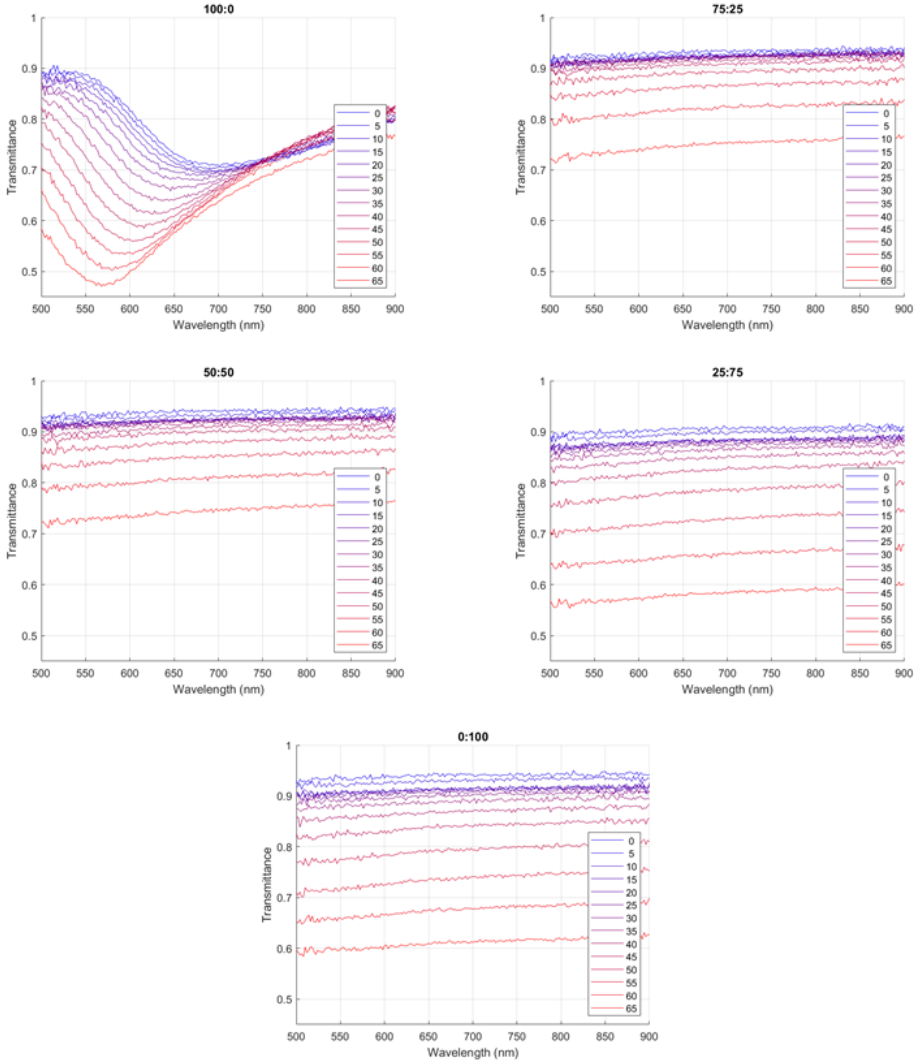

Figure 13. Angle dependent transmittance of CNC:CNF samples. 100:0 has a distinctive reflectance pattern due to CNC iridescence. Reproduced with permission under Creative Commons license CC-BY [96]

Based on the result of **Publications II and III**, while films including CNF show interesting mechanical properties, their overall optics and surface roughness make unmodified CNF an unsuitable material for optoelectronics substrates. CNC films, on the other hand, show some potential as their roughness is quite low and their reflectivity can be eliminated.

Cellulose has potential, but requires many modifications to compete with the currently used substrate materials. The films are already highly transparent and require minimal surface roughness reduction, yet, going forward other problems will arise – cellulose unfavorable interactions with water and other solvents need to be reduced to prevent swelling and redispersion, and cellulose poor gas barrier levels need to be improved to reduce the perovskite degradation. These problems and possible solutions are further explored in **Publication V**.

4.2 How cellulose and PSC fabrication can be combined (Publications IV and V)

4.2.1 Simplifying perovskite solar cell fabrication for materials testing: how to use unetched substrates with the aid of a three-dimensionally printed cell holder

I wrote **Publication IV** anticipating the adoption of cellulose as a substrate for PSCs. Two steps of the PSC fabrication and characterization could pose problems for cellulose: etching of the bottom electrode and connecting the electrodes to instruments for IV and IS characterization.

Solar cells require light to reach the active area to generate a photocurrent, therefore, to make the most of the available irradiation, the layers between the active area and the outside of the cells have to be as transparent as possible. On the other hand, the electrode resistivity and transmittance decrease with thickness. Therefore, there is a trade-off between the electrode transmittance and the sheet resistance, usually expressed as its figure-of-merit (FOM). While useful, FOM is a very general unit that does not consider the wavelengths that are used by the solar cell, nor does it consider the length between the area where the photocurrent is generated and where the transparent electrode and the cabling join. Anand et al. introduced a novel FOM to fix this issue [97], and with this new metric they found that for solar cells with a wavelength range between 350-800 nm, only dielectric/metal/dielectric composite electrodes, metallic nanowires and meshes, and one organic polymer have similar FOM to ITO and FTO. Coincidentally, these electrodes are compatible with cellulose films, showing that it is possible to replace TCOs while maintaining a high transparency and conductivity ratio.

The main purpose of etching TCO from the substrate is to create sections where the top electrode can be deposited without short circuiting the cell. In a laboratory scale, TCO is chemically etched from the substrate using zinc powder and diluted acid solution. In the case of cellulose films, I anticipate that metallic nanowires would be electrode material of choice. While metallic nanowires can reach high

FOM values, they can increase the surface roughness, complicating the deposition of subsequent layers. A way to reduce this is by embedding the nanowires into the cellulose matrix, leveling the nanowires with the cellulose while keeping the nanowire network. However, after this step the nanowires cannot be etched. In an industrial setting, this could be overcome by spraying the nanowires with the help of stencil patterns, yet, it is difficult to reach this level of production if the problem is not solved at a small scale.

The second issue is connecting the electrodes to characterization instruments. Normally in a laboratory scale, alligator clamps and silver ink are used to connect PSCs to a potentiostat to perform IV and EIS measurements under a solar simulator. Silver ink is used as a semisoft coating on top of the electrode to make good contact with the alligator clamp. This approach poses two problems for cellulose films. The first and most obvious, is that clamps can damage the substrate and scratch of the electrode, and are limited to certain regions of the cell they can touch. The second problem is that the silver ink is in a solvent that could affect cellulose or the PSC, and as it tends to diffuse into the electrode, it would short circuit an unetched substrate.

These problems were solved by making a custom solar cell holder that allows any part of the cell to be contacted with constant pressure (**Figure 7**). The holder was 3D printed as it allows for easy prototyping. To connect the cell to the characterization instruments, spring-loaded pins that keep a constant pressure on the substrate without damaging it were used. To test our holder, PSCs were made on etched and unetched glass/FTO substrates and characterized. The results showed that there is no significant difference between etched and unetched substrates, independently of measurement location on the cell (**Table 3**). This article resulted in an easily implemented characterization tool, ready for flexible solar cells on cellulose.

Table 3. Results from PSCs made on etched and unetched substrates. Reproduced from Publication IV with permission under Creative Commons Attribution License 4.0 [82]

DEVICE	NUMBER OF PIXELS	*H* (%)	J_{SC} (MA/CM^2)	V_{OC} (V)	*FF* (%)
FOUR-PIXEL GROUP					
EDGE ETCHED	24	16.0 ± 0.7	22.1 ± 0.8	1.02 ± 0.03	71 ± 2
EDGE UNETCHED	24	16 ± 1	22.9 ± 0.8	1.01 ± 0.02	71 ± 3
CENTRE UNETCHED	24	16 ± 2	23.1 ± 0.4	1.01 ± 0.02	72 ± 3
EIGHT-PIXEL GROUP					
EDGE ETCHED	47	14 ± 2	18.7 ± 0.9	1.12 ± 0.02	68 ± 5
CENTRE UNETCHED	48	15 ± 2	19 ± 2	1.11 ± 0.02	72 ± 4

4.2.2 Combining cellulose substrates and perovskites in sustainable solar cells is possible: a systematic literature review with realistic solutions

In **Publication V**, I developed a wide strategy to adapt cellulose for use in PSCs. To be considered a suitable substrate alternative, cellulose films need to have the following properties [18]:

- Flexibility, at least enough to resist roll-to-roll (R2R) fabrication processes
- Thermal tolerance, to resist the thermal annealing processes during the solar cell fabrication
- Good optical transmittance, so most of the usable light reaches the solar cell active area
- Low thermal expansion, to avoid expanding and damaging the layers deposited on top
- High electrical conductivity, to minimize resistive energy loses
- Very low surface roughness, to ensure the proper deposition of the layers that make the device
- Resistance to solvents, since wet deposition methods depend on using a wide variety of solvents
- Very low oxygen and water vapor permeation, to minimize the solar cell degradation

Some types of cellulose can be inherently brittle; one way to improve the flexibility of cellulose films is through the addition of plasticizers; small molecules situated between cellulose chains that disrupt inter-chain hydrogen bonding, increasing their molecular mobility [98]. Due to cellulose intra- and inter-molecule bonding, cellulose can resist higher temperatures than PET and PEN without melting. Nonetheless, additional features such as increased flexibility can be lost at temperatures higher than 100 °C as plasticizers degrade [99]. If the device that is to be made on top of the cellulose substrate does not require annealing temperatures over 100 °C, then plasticizers such as glycerol can used; otherwise, crosslinking would be required to reach temperatures close to 300 °C [50]. Moreover, while the mechanical properties of cellulose films are sometimes reported, there is no clear standard as they are highly machine- and instrument-dependent, so the only clear guideline is that cellulose needs to be “flexible enough” for however solar cells are made.

One often overlooked aspect when discussing substrate materials is the coefficient of thermal expansion (*CTE*). Typical fabrication processes tend to involve thermal annealing steps to remove solvents and sinter ceramic layers. As materials are heated, they expand at different rates, and this effect can cause fractures

and other defects. Cellulose *CTE* depends on the direction of the cellulose chains [100], and it is also affected by crosslinking [101].

One of the most important properties of a substrate is its transparency. The more light reaches the active material, the higher the photocurrent generated, given that the light is of the proper wavelength. Cellulose films' transparency is strongly influenced by drying conditions that need to be carefully controlled. In the case of cellulose acetate films prepared for **Publication V**, the relative humidity and the concentration have to be controlled to avoid the cellulose chains to form a porous structure that highly scatters light, effectively making the film opaque. In the case of CNC, the chiral nematic structure that gives rise to the iridescent look of the films can be eliminated by ultrasonicating the CNC while still in suspension to further break down the nanocrystals, shifting the reflection to the infrared part of the spectrum, or by introducing a crosslinker or a plasticizer that modifies how the cellulose chains settle.

As discussed earlier, there is a trade-off between transparency and electrode conductivity. Metallic nanowires are easy to adapt to cellulose and have FOM similar to that of TCOs. One consideration here is that nanowires need to be embedded in the cellulose matrix to reduce the substrate surface roughness, as this can negatively affect the deposition of the other layers. Although surface roughness is less of an issue using polymeric electrodes, it is at the expense of a lower FOM.

PSC fabrication usually involves wet methods for layer deposition. These methods require using a variety of solvents that may redisperse the cellulose substrate. To solve this issue (i) a type of cellulose that inherently solvent-resistance can be used, (ii) cellulose can be crosslinked to make the film solvent resistant, (iii) the solvents used can be replaced for others that do not affect the film, or a combination of these three options. Finally, the films require high gas barrier levels to avoid oxygen and water to enter and degrade the layers of the device. Considering all these factors, I developed a realistic strategy to adapt cellulose films and the PSC fabrication methods to work together (**Figure 14**). One thing that is worth mentioning is that the values required, for example, flexibility and CTE, are hard to define. The necessary flexibility is unclear, as this is very process and machine dependent, the desired CTE can change depending on the CTE of the layers deposited on the substrate, and the acceptable surface roughness depends on the type of material and thickness of the first deposited layers. At this point, a good guideline is that cellulose films need to have mechanical and morphological properties similar to already used materials like PET and PEN. This similarity would facilitate the exploration of biobased substrates through well-established fabrication protocols.

The 1st step is to modify cellulose while it is still in suspension/solution. By crosslinking, the resulting films can gain enough solvent resistance and a small improvement in gas barrier properties, and adding a plasticizer can provide enough flexibility to endure the fabrication process. The 2nd step requires controlling the

drying conditions to achieve the highest possible transparency, and for the film to be dried on a very smooth surface to reduce the film surface roughness. After the film is dry it needs to be coated to reduce its oxygen transmission rate (OTR), its WVTR, and it also works as a planarization layer to further reduce the surface roughness. The 4th step involves attaching the film to a rigid carrier, in case the process is carried out in a small laboratory scale. Then the electrode material is deposited, be it metallic nanowires or a conductive polymer. Next, the substrate needs to be cleaned. Unlike the traditional route on glass substrates, cellulose cannot be cleaned used a solvent sonication bath, and UV-O_3 is discouraged as it can negatively affect cellulose by breaking organic bonds. Instead, it is better to clean the surface quickly by dynamically spin coating a compatible solvent on the surface, or using plasma and a web cleaner in the case of a R2R process. In the 5th step, the substrate needs to allow for the easy spread of the next layer over the electrode. This can be done using a low power plasma to modify the wettability of the surface of the film, or by adding a surfactant to lower the surface tension of the ink.

In the 6th step, solvents play an important role. The solvent of the first CTL will have a big impact on the cellulose film, as there can be little in the way protecting the substrate. Here the cellulose can have some solvent resistance thanks to the crosslinking earlier, but also by carefully selecting a solvent that is compatible with the substrate. Usually, in the 7th step there is a thermal annealing step to remove the solvent and crystallize the CTL. The thermal treatment can be avoided using different strategies, depending on the CTL material. This is to avoid cellulose buckling due to moisture loss or damage done because of the different *CTEs* of each layer.

In the 8th step there is the perovskite deposition. Here, similar to step 6, the solvent choice is also important, and how to use different antisolvents, or skip them completely. Step 9 is similar to 7, as there are ways to avoid the thermal annealing of the perovskite. Step 10 also requires solvents to be considered to deposit the second CTL. Finally, the top electrode can be laminated or mechanically pressed on the cell to avoid evaporation-based deposition, which could damage the cell.

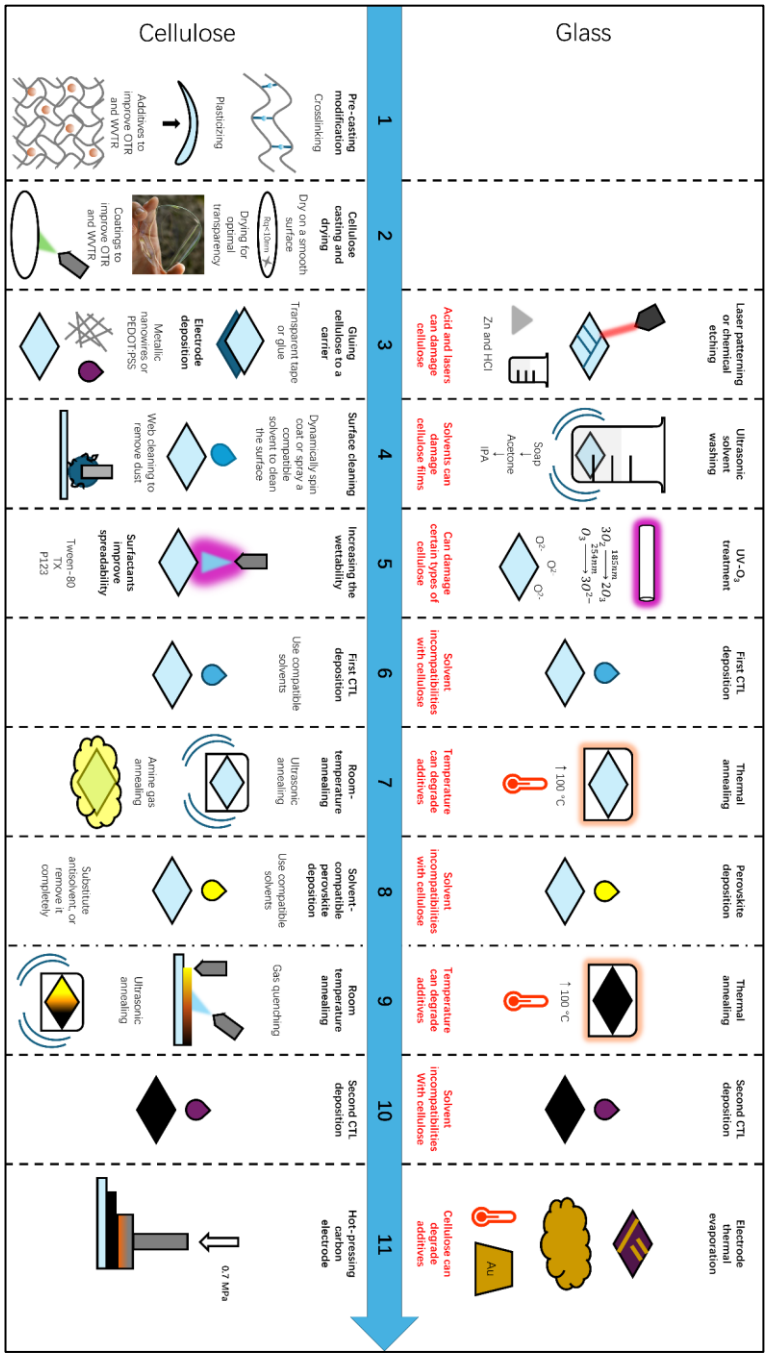

Figure 14. 11 steps to make PSCs on cellulose substrates

5 Conclusions and outlook

5.1 Summary and conclusions

This work examines the integration of cellulose in PSCs to increase their sustainability. The research discusses how cellulose can be modified to more closely adopt the properties of the currently used substrate materials in optoelectronics, how PSC fabrication can be modified to fit cellulose limitations, and how eventually cells made on cellulose could be characterized. This chapter summarizes the results from each publication and how they answer the research questions from Chapter 1.

5.1.1 Bio-based materials and PSCs: a mutually beneficial relationship

Publication I concludes that cellulose is a promising bio-based material that could improve the recyclability of PSCs. Unfortunately, unlike carbon-based electrodes which are already well-established in solar cell architectures, cellulose-based components are still in an early research stage. As stated there, one of the major hurdles of recycling photovoltaic devices is the low profitability of the process. 47% of the material value in a silicon solar panel is in the silver contacts when they are only 0.1% of the weight – recovering this material is key to attract capital to recycle solar panels. One of the biggest obstacles to recycling is the substrate as it represents most of the weight and "dilutes" the value of the panel. Cellulose has potential to replace glass and other polymers and improve the recyclability of PSCs compared to silicon cells, but it requires modifications.

Publication II demonstrated that CNF suspensions can be adjusted to produce films with significantly different surface morphology, mechanical and optical properties, and how the nanofibril size played a major role in the film quality even when using different CNF grades. **Publication III** presented strategies to reduce water uptake and improve the mechanical properties of the films; however, it was observed that while CNF increases the flexibility of CNC films, it does so at the expense of a significant increase in surface roughness. The inclusion of MTM

nanoclay in the films slightly reduced the water swelling and WVTR, but this also came with the downside of reducing the optical transmittance and flexibility of the films, and an increase complexity to fabricate and handle them.

Different solutions were explored in **Publication V** to address the limitations encountered in **Publications II and III**. The first thing to do was to examine the properties that make for an appropriate substrate material, and comparing cellulose to what is currently being used. Next, modifications and treatments that can be done to cellulose to reach acceptable levels of transparency, surface roughness, flexibility, and solvent resistance, among others, were discussed. We conclude that cellulose requires (i) to be crosslinked to prevent it from swelling and redispersionin solvents, and to slightly increase its gas barrier properties, (ii) the inclusion of plasticizers for improved flexibility, (iii) careful control of its drying conditions to achieve maximum transparency and surface smoothness, and (iv) coatings to further reduce its OTR and WVTR.

5.1.2 Combining PSCs and cellulose: a method

After obtaining proper cellulose substrates made in the first steps laid out in **Publication V**, the PSC fabrication route needs to be revised and adapted to work within the constraints posed by cellulose. First, UV-O_3 can damage and make the substrate too hydrophilic – surfactants can increase ink spreadability; plasma can help with this and clean the surface too. Next, solvents need to be considered and replaced with alternatives that are compatible with the substrate, favoring green alternatives. Additionally, thermal annealing needs to be replaced with room or low temperatures approaches, such as ultrasonication or gas quenching. Finally, the top electrode, usually made with precious metals, needs to be replaced with carbon or a film with metallic nanowires to maintain a minimum environmental impact.

Anticipating their eventual development, **Publication IV** explored solar cells on cellulose as they require some attentions during characterization. One of my worries is that researchers exploring cellulose substrates in their devices will treat solar cells made on cellulose like their rigid counterparts, and will dismiss this material because they did not consider it has different requirements. In the first stages of development, solar cells on cellulose will be fabricated in a small scale and attached to a rigid substrate, where it is possible to use the designed holder. Later on, as cellulose proves to be a viable alternative, more methods can be developed, as it happened when PET and PEN were first tested.

5.2 Future work

A crucial step to make cellulose a material PSC researchers consider is to ease the transition to this type of substrate. Once proper cellulose film has been developed, it needs to report it has the properties a PSC requires of a substrate to be taken seriously: good gas barrier levels, very low surface roughness, high transparency, and what solvents it is compatible with. Only some of these values are reported in the literature, as research teams focus on tackling only specific issues. Nonetheless, reporting all these values is essential. It is understandable that not everything is reported, as this can be due to time constraints or lack of infrastructure; however, this is an indication that more collaboration between research teams is needed to promote cellulose as a sustainable alternative to glass and synthetic polymers. Another way that would help cellulose researchers developing these films would be to remind PSC researchers of the different fabrication methods they can use – flexibility and innovation on their part would greatly help circumvent cellulose's limitations.

There are four things that I think are needed soon after solar cells on cellulose become a reality: A life-cycle assessment, aging and degradation tests, proper biobased encapsulation, and the development of a recycling methodology. As it has been stated throughout this work, cellulose can increase solar cell sustainability, but we need numbers to support these claims, and to my knowledge, no studies have yet addressed this topic. Once these cells are made, they need to be aged to see their particular degradation patterns and how they fare against other substrate materials. Furthermore, to assure longtime performance but maintain their sustainability, these cells need to be paired with biobased encapsulants; it would be a shame to develop these cells to have them encapsulated between glass and an epoxy resin. Finally, we need proof that valuable materials can be easily recovered with this architecture and compare it to the state-of-the-art technologies. As always, there is a lot more work to be done, all in hope of finally achieving truly renewable energy source.

List of References

[1] J. Lelieveld, K. Klingmüller, A. Pozzer, R. T. Burnett, A. Haines, and V. Ramanathan, "Effects of fossil fuel and total anthropogenic emission removal on public health and climate," *Proceedings of the National Academy of Sciences*, vol. 116, no. 15, pp. 7192–7197, Apr. 2019, doi: 10.1073/pnas.1819989116.

[2] M. G. Barron, D. N. Vivian, R. A. Heintz, and U. H. Yim, "Long-Term Ecological Impacts from Oil Spills: Comparison of Exxon Valdez, Hebei Spirit, and Deepwater Horizon," *Environ Sci Technol*, vol. 54, no. 11, pp. 6456–6467, Jun. 2020, doi: 10.1021/acs.est.9b05020.

[3] T. Xia, Q. Ji, D. Zhang, and J. Han, "Asymmetric and extreme influence of energy price changes on renewable energy stock performance," *J Clean Prod*, vol. 241, p. 118338, Dec. 2019, doi: 10.1016/j.jclepro.2019.118338.

[4] J. Ko, H. F. Lee, and C. K. Leung, "War and warming: The effects of climate change on military conflicts in developing countries (1995–2020)," *Innovation and Green Development*, vol. 3, no. 4, p. 100175, Dec. 2024, doi: 10.1016/j.igd.2024.100175.

[5] B. J. van Ruijven, E. De Cian, and I. Sue Wing, "Amplification of future energy demand growth due to climate change," *Nat Commun*, vol. 10, no. 1, p. 2762, Jun. 2019, doi: 10.1038/s41467-019-10399-3.

[6] A. Saxena, C. Brown, A. Arneth, and M. Rounsevell, "Modelling the global photovoltaic potential on land and its sensitivity to climate change," *Environmental Research Letters*, vol. 18, no. 10, p. 104017, Oct. 2023, doi: 10.1088/1748-9326/acf86f.

[7] "Renewable capacity statistics 2024," Abu Dhabi, 2024. Accessed: Nov. 07, 2024. [Online]. Available: https://www.irena.org/-/media/Files/IRENA/Agency/Publication/2024/Mar/IRENA_RE_Capacity_Statistics_2024.pdf

[8] G. Masson, M. de l'Epine, I. Kaizuka, and J. Okazaki, "Trends in PV Applications 2025," 2025. doi: 10.69766/NCNN2417.

[9] A. Jäger-Waldau, "Snapshot of Photovoltaics − May 2023," *EPJ Photovoltaics*, vol. 14, p. 23, Jul. 2023, doi: 10.1051/epjpv/2023016.

[10] IEA (2023), "Renewable Energy Market Update - June 2023," Paris, 2023. Accessed: Nov. 11, 2024. [Online]. Available: https://www.iea.org/reports/renewable-energy-market-update-june-2023

[11] BloombergNEF, "3Q 2024 Global PV Market Outlook," 2024. Accessed: Nov. 11, 2024. [Online]. Available: https://about.bnef.com/blog/3q-2024-global-pv-market-outlook/

[12] S. Preet and S. T. Smith, "A comprehensive review on the recycling technology of silicon based photovoltaic solar panels: Challenges and future outlook," *J Clean Prod*, vol. 448, p. 141661, Apr. 2024, doi: 10.1016/j.jclepro.2024.141661.

[13] G. A. Heath *et al.*, "Research and development priorities for silicon photovoltaic module recycling to support a circular economy," *Nat Energy*, vol. 5, no. 7, pp. 502–510, Jul. 2020, doi: 10.1038/s41560-020-0645-2.

[14] B. Hallam *et al.*, "The silver learning curve for photovoltaics and projected silver demand for net-zero emissions by 2050," *Progress in Photovoltaics: Research and Applications*, vol. 31, no. 6, pp. 598–606, Jun. 2023, doi: 10.1002/pip.3661.

[15] M. Tao *et al.*, "Major challenges and opportunities in silicon solar module recycling," *Progress in Photovoltaics: Research and Applications*, vol. 28, no. 10, pp. 1077–1088, Oct. 2020, doi: 10.1002/pip.3316.

[16] X. Wang, X. Tian, X. Chen, L. Ren, and C. Geng, "A review of end-of-life crystalline silicon solar photovoltaic panel recycling technology," *Solar Energy Materials and Solar Cells*, vol. 248, p. 111976, Dec. 2022, doi: 10.1016/j.solmat.2022.111976.

[17] S. Kim, H. Van Quy, and C. W. Bark, "Photovoltaic technologies for flexible solar cells: beyond silicon," *Mater Today Energy*, vol. 19, p. 100583, Mar. 2021, doi: 10.1016/j.mtener.2020.100583.

[18] P. Subudhi and D. Punetha, "Progress, challenges, and perspectives on polymer substrates for emerging flexible solar cells: A holistic panoramic review," *Progress in Photovoltaics: Research and Applications*, vol. 31, no. 8, pp. 753–789, Aug. 2023, doi: 10.1002/pip.3703.

[19] X. Li, P. Li, Z. Wu, D. Luo, H.-Y. Yu, and Z.-H. Lu, "Review and perspective of materials for flexible solar cells," *Materials Reports: Energy*, vol. 1, no. 1, p. 100001, Feb. 2021, doi: 10.1016/j.matre.2020.09.001.

[20] V. Volpe, M. S. Lanzillo, A. Molaro, G. Affinita, and R. Pantani, "Characterization of Recycled/Virgin Polyethylene Terephthalate Composite Reinforced with Glass Fiber for Automotive Applications," *Journal of Composites Science*, vol. 6, no. 2, p. 59, Feb. 2022, doi: 10.3390/jcs6020059.

[21] L. Viora *et al.*, "A Comparative Study on Crystallisation for Virgin and Recycled Polyethylene Terephthalate (PET): Multiscale Effects on Physico-Mechanical Properties," *Polymers (Basel)*, vol. 15, no. 23, p. 4613, Dec. 2023, doi: 10.3390/polym15234613.

[22] M. Davis and Z. Yu, "A review of flexible halide perovskite solar cells towards scalable manufacturing and environmental sustainability," *Journal of Semiconductors*, vol. 41, no. 4, p. 041603, Apr. 2020, doi: 10.1088/1674-4926/41/4/041603.

[23] H. Qi, *Novel Functional Materials Based on Cellulose*. in SpringerBriefs in Applied Sciences and Technology. Cham: Springer International Publishing, 2017. doi: 10.1007/978-3-319-49592-7.

[24] X. Ma *et al.*, "Cellulose transparent conductive film and its feasible use in perovskite solar cells," *RSC Adv*, vol. 9, no. 17, pp. 9348–9353, 2019, doi: 10.1039/C9RA01301F.

[25] D. Gounden, M. N. Pillay, V. Moodley, N. Nombona, and W. E. van Zyl, "Fabrication and processing of bacterial cellulose/silver nanowire composites as transparent, conductive, and flexible films for optoelectronic applications," *J Appl Polym Sci*, vol. 140, no. 30, Aug. 2023, doi: 10.1002/app.54090.

[26] X. Xu *et al.*, "Highly transparent, low-haze, hybrid cellulose nanopaper as electrodes for flexible electronics," *Nanoscale*, vol. 8, no. 24, pp. 12294–12306, 2016, doi: 10.1039/C6NR02245F.

[27] X. Sun *et al.*, "Nanocellulose films with combined cellulose nanofibers and nanocrystals: tailored thermal, optical and mechanical properties," *Cellulose*, vol. 25, no. 2, pp. 1103–1115, Feb. 2018, doi: 10.1007/s10570-017-1627-9.

[28] F. D'Acierno, C. A. Michal, and M. J. MacLachlan, "Thermal Stability of Cellulose Nanomaterials," *Chem Rev*, vol. 123, no. 11, pp. 7295–7325, Jun. 2023, doi: 10.1021/acs.chemrev.2c00816.

[29] A. M. Salem, A. R. Mohamed, A. M. Abdelghany, and A. Y. Yassin, "Effect of polypyrrole on structural, optical and thermal properties of CMC-based blends for optoelectronic applications," *Opt Mater (Amst)*, vol. 134, p. 113128, Dec. 2022, doi: 10.1016/j.optmat.2022.113128.

[30] G. Wypych, "Handbook of Polymers (3rd Edition)," *ChemTec Publishing*. [Online]. Available: https://app.knovel.com/hotlink/toc/id:kpHPE00045/handbook-polymers-3rd/handbook-polymers-3rd

[31] L. H. Lalasari, T. Arini, L. Andriyah, F. Firdiyono, and A. H. Yuwono, "Electrical, optical and structural properties of FTO thin films fabricated by spray ultrasonic nebulizer technique from SnCl4 precursor," 2018, p. 020001. doi: 10.1063/1.5038283.

[32] W.-F. Wu and B.-S. Chiou, "Effect of annealing on electrical and optical properties of RF magnetron sputtered indium tin oxide films," *Appl Surf Sci*, vol. 68, no. 4, pp. 497–504, Aug. 1993, doi: 10.1016/0169-4332(93)90233-2.

[33] I. López-Fernández *et al.*, "Lead-Free Halide Perovskite Materials and Optoelectronic Devices: Progress and Prospective," *Adv Funct Mater*, vol. 34, no. 6, Feb. 2024, doi: 10.1002/adfm.202307896.

[34] A. Kojima, K. Teshima, Y. Shirai, and T. Miyasaka, "Organometal Halide Perovskites as Visible-Light Sensitizers for Photovoltaic Cells," *J Am Chem Soc*, vol. 131, no. 17, pp. 6050–6051, May 2009, doi: 10.1021/ja809598r.

[35] M. A. Green *et al.*, "Solar cell efficiency tables (Version 64)," *Progress in Photovoltaics: Research and Applications*, vol. 32, no. 7, pp. 425–441, Jul. 2024, doi: 10.1002/pip.3831.

[36] J. J. Kaschuk *et al.*, "Processing factors affecting roughness, optical and mechanical properties of nanocellulose films for optoelectronics," *Carbohydr Polym*, vol. 332, p. 121877, May 2024, doi: 10.1016/j.carbpol.2024.121877.

[37] M. K. Bin Bakri, M. R. Rahman, and F. I. Chowdhury, "Sources of cellulose," in *Fundamentals and Recent Advances in Nanocomposites Based on Polymers and Nanocellulose*, Elsevier, 2022, pp. 1–18. doi: 10.1016/B978-0-323-85771-0.00012-9.

[38] O. A. El Seoud, M. Kostag, K. Jedvert, and N. I. Malek, "Cellulose Regeneration and Chemical Recycling: Closing the 'Cellulose Gap' Using Environmentally Benign Solvents," *Macromol Mater Eng*, vol. 305, no. 4, Apr. 2020, doi: 10.1002/mame.201900832.

[39] A. Forte, F. Dourado, A. Mota, B. Neto, M. Gama, and E. C. Ferreira, "Life cycle assessment of bacterial cellulose production," *Int J Life Cycle Assess*, vol. 26, no. 5, pp. 864–878, May 2021, doi: 10.1007/s11367-021-01904-2.

[40] Z. Yuan *et al.*, "Heterogeneous strategies for selective conversion of lignocellulosic polysaccharides," *Cellulose*, vol. 29, no. 6, pp. 3059–3077, Apr. 2022, doi: 10.1007/s10570-022-04434-8.

[41] M. Reimer and C. Zollfrank, "Cellulose for Light Manipulation: Methods, Applications, and Prospects," *Adv Energy Mater*, vol. 11, no. 43, Nov. 2021, doi: 10.1002/aenm.202003866.

[42] Y. Li, Q. Fu, X. Yang, and L. Berglund, "Transparent wood for functional and structural applications," *Philosophical Transactions of the Royal Society A: Mathematical, Physical and Engineering Sciences*, vol. 376, no. 2112, p. 20170182, Feb. 2018, doi: 10.1098/rsta.2017.0182.

[43] M. Ghasemi, M. Tsianou, and P. Alexandridis, "Assessment of solvents for cellulose dissolution," *Bioresour Technol*, vol. 228, pp. 330–338, Mar. 2017, doi: 10.1016/j.biortech.2016.12.049.

[44] Z. Liu *et al.*, "Characterization of the regenerated cellulose films in ionic liquids and rheological properties of the solutions," *Mater Chem Phys*, vol. 128, no. 1–2, pp. 220–227, Jul. 2011, doi: 10.1016/j.matchemphys.2011.02.062.

[45] W. Zhu *et al.*, "Aligned regenerated cellulose films with enhanced mechanical and optical properties for light management," *Colloids Surf A Physicochem Eng Asp*, vol. 674, p. 131985, Oct. 2023, doi: 10.1016/j.colsurfa.2023.131985.

[46] I. S. Makarov *et al.*, "Structure, Morphology, and Permeability of Cellulose Films," *Membranes (Basel)*, vol. 12, no. 3, p. 297, Mar. 2022, doi: 10.3390/membranes12030297.

[47] N. B. Erdal and M. Hakkarainen, "Degradation of Cellulose Derivatives in Laboratory, Man-Made, and Natural Environments," *Biomacromolecules*, vol. 23, no. 7, pp. 2713–2729, Jul. 2022, doi: 10.1021/acs.biomac.2c00336.

[48] S. Castro-Hermosa, J. Dagar, A. Marsella, and T. M. Brown, "Perovskite solar cells on paper and the role of substrates and electrodes on performance," *IEEE Electron Device Letters*, vol. 38, no. 9, pp. 1278–1281, Sep. 2017, doi: 10.1109/LED.2017.2735178.

[49] Z. Xiao *et al.*, "Ultra-flexible organic solar cells based on eco-friendly cellulose substrate with efficiency approaching 19%," *J Mater Chem A Mater*, vol. 13, no. 3, pp. 2301–2308, 2025, doi: 10.1039/D4TA07622B.

[50] L. Huang, Y. Li, Z. Zheng, Y. Bai, T. P. Russell, and C. He, "Flexible, transparent, and sustainable cellulose-based films for organic solar cell substrates," *Mater Horiz*, vol. 11, no. 6, pp. 1560–1566, 2024, doi: 10.1039/D3MH01998E.

[51] NREL, "Best Research-Cell Efficiency Chart." Accessed: May 05, 2025. [Online]. Available: https://www2.nrel.gov/pv/cell-efficiency

[52] A. Hassan *et al.*, "Unveiling the potential of flexible perovskite photovoltaics: From lab to fab," *Materials Science and Engineering: R: Reports*, vol. 166, p. 101023, Sep. 2025, doi: 10.1016/j.mser.2025.101023.

[53] J. Lee, B. S. Kim, J. Park, J. Lee, and K. Kim, "Opportunities and Challenges for Perovskite Solar Cells Based on Vacuum Thermal Evaporation," *Adv Mater Technol*, vol. 8, no. 20, Oct. 2023, doi: 10.1002/admt.202200928.

[54] E. Aydin *et al.*, "Pathways toward commercial perovskite/silicon tandem photovoltaics," *Science (1979)*, vol. 383, no. 6679, Jan. 2024, doi: 10.1126/science.adh3849.

[55] S. Bello, A. Urwick, F. Bastianini, A. J. Nedoma, and A. Dunbar, "An introduction to perovskites for solar cells and their characterisation," *Energy Reports*, vol. 8, pp. 89–106, Nov. 2022, doi: 10.1016/j.egyr.2022.08.205.

[56] S. Tao *et al.*, "Absolute energy level positions in tin- and lead-based halide perovskites," *Nat Commun*, vol. 10, no. 1, p. 2560, Jun. 2019, doi: 10.1038/s41467-019-10468-7.

[57] Y. Liang *et al.*, "Toward stabilization of formamidinium lead iodide perovskites by defect control and composition engineering," *Nat Commun*, vol. 15, no. 1, p. 1707, Feb. 2024, doi: 10.1038/s41467-024-46044-x.

[58] N. Ahn and M. Choi, "Towards Long-Term Stable Perovskite Solar Cells: Degradation Mechanisms and Stabilization Techniques," *Advanced Science*, vol. 11, no. 4, Jan. 2024, doi: 10.1002/advs.202306110.

[59] L. Liu *et al.*, "A-site phase segregation in mixed cation perovskite," *Materials Reports: Energy*, vol. 1, no. 4, p. 100064, Nov. 2021, doi: 10.1016/j.matre.2021.100064.

[60] K. E. Gkini, M. Antoniadou, N. Balis, A. Kaltzoglou, A. G. Kontos, and P. Falaras, "Mixing cations and halide anions in perovskite solar cells," *Mater Today Proc*, vol. 19, pp. 73–78, 2019, doi: 10.1016/j.matpr.2019.07.660.

[61] H. Dong *et al.*, "Annealing-Free, High-Performance Perovskite Solar Cells by Controlling Crystallization via Guanidinium Cation Doping," *Solar RRL*, vol. 5, no. 7, Jul. 2021, doi: 10.1002/solr.202100097.

[62] K. Sakhatskyi *et al.*, "Assessing the Drawbacks and Benefits of Ion Migration in Lead Halide Perovskites," *ACS Energy Lett*, vol. 7, no. 10, pp. 3401–3414, Oct. 2022, doi: 10.1021/acsenergylett.2c01663.

[63] H. F. Zarick, N. Soetan, W. R. Erwin, and R. Bardhan, "Mixed halide hybrid perovskites: a paradigm shift in photovoltaics," *J Mater Chem A Mater*, vol. 6, no. 14, pp. 5507–5537, 2018, doi: 10.1039/C7TA09122B.

[64] T. Jesper Jacobsson *et al.*, "Exploration of the compositional space for mixed lead halogen perovskites for high efficiency solar cells," *Energy Environ Sci*, vol. 9, no. 5, pp. 1706–1724, 2016, doi: 10.1039/C6EE00030D.

[65] C. Jing, Z. Lin, Y. Wu, and X. Ouyang, "Air-Processed Perovskite Solar Cells: Challenges, Progress, and Industrial Strategies," *Small*, vol. 21, no. 35, Sep. 2025, doi: 10.1002/smll.202504448.

[66] A. Ummadisingu *et al.*, "The effect of illumination on the formation of metal halide perovskite films," *Nature*, vol. 545, no. 7653, pp. 208–212, May 2017, doi: 10.1038/nature22072.

[67] G. Bartholazzi, R. P. Pereira, A. M. Lima, W. A. Pinheiro, and L. R. Cruz, "Influence of substrate temperature on the chemical, microstructural and optical properties of spray deposited CH3NH3PbI3 perovskite thin films," *Journal of Materials Research and Technology*, vol. 9, no. 3, pp. 3411–3417, May 2020, doi: 10.1016/j.jmrt.2020.01.078.

[68] R. Kang, J.-E. Kim, J.-S. Yeo, S. Lee, Y.-J. Jeon, and D.-Y. Kim, "Optimized Organometal Halide Perovskite Planar Hybrid Solar Cells via Control of Solvent Evaporation Rate," *The Journal of Physical Chemistry C*, vol. 118, no. 46, pp. 26513–26520, Nov. 2014, doi: 10.1021/jp508015c.

[69] E. Climent-Pascual *et al.*, "Influence of the substrate on the bulk properties of hybrid lead halide perovskite films," *J Mater Chem A Mater*, vol. 4, no. 46, pp. 18153–18163, 2016, doi: 10.1039/C6TA08695K.

[70] W. Ke *et al.*, "Efficient hole-blocking layer-free planar halide perovskite thin-film solar cells," *Nat Commun*, vol. 6, no. 1, p. 6700, Mar. 2015, doi: 10.1038/ncomms7700.

[71] X. Cai *et al.*, "A review for nickel oxide hole transport layer and its application in halide perovskite solar cells," *Materials Today Sustainability*, vol. 23, p. 100438, Sep. 2023, doi: 10.1016/j.mtsust.2023.100438.

[72] A. Nayfeh and S. Abdul Hadi, "Basics of solar cells," in *Silicon-Germanium Alloys for Photovoltaic Applications*, Elsevier, 2023, pp. 17–35. doi: 10.1016/B978-0-323-85630-0.00004-2.

[73] E. S. Oh, S. Lee, S. Y. Oh, Z. Guo, and G. M. Kim, "Reduction of fabrication time for organic–inorganic hybrid perovskite solar cells in lab-scale," *Solar Energy*, vol. 278, p. 112793, Aug. 2024, doi: 10.1016/j.solener.2024.112793.

[74] S. Foo, M. Thambidurai, P. Senthil Kumar, R. Yuvakkumar, Y. Huang, and C. Dang, "Recent review on electron transport layers in perovskite solar cells," *Int J Energy Res*, vol. 46, no. 15, pp. 21441–21451, Dec. 2022, doi: 10.1002/er.7958.

[75] X. Liu, J. Gong, B. Xue, T. Bu, Y. Cheng, and F. Huang, "Inorganic Charge Transport Layers for High-Performance p-i-n Perovskite Solar Cells," *ChemSusChem*, Nov. 2025, doi: 10.1002/cssc.202501739.

[76] H. C. Weerasinghe *et al.*, "The first demonstration of entirely roll-to-roll fabricated perovskite solar cell modules under ambient room conditions," *Nat Commun*, vol. 15, no. 1, p. 1656, Mar. 2024, doi: 10.1038/s41467-024-46016-1.

[77] S. Chaudhary, S. K. Gupta, and C. M. Singh Negi, "Enhanced performance of perovskite photodetectors fabricated by two-step spin coating approach," *Mater Sci Semicond Process*, vol. 109, p. 104916, Apr. 2020, doi: 10.1016/j.mssp.2020.104916.

[78] P. Eaton and P. West, *Atomic Force Microscopy*. Oxford University Press, 2010. doi: 10.1557/mrs.2014.72.

[79] N. D. Sankir and M. Sankir, *Printable Solar Cells*. Newark, UNITED STATES: John Wiley & Sons, Incorporated, 2017. [Online]. Available: http://ebookcentral.proquest.com/lib/kutu/detail.action?docID=4845195

[80] P. M. Schweizer and S. F. Kistler, *Liquid Film Coating : Scientific Principles and Their Technological Implications*. Dordrecht, NETHERLANDS, THE: Springer Netherlands, 1997. [Online]. Available: http://ebookcentral.proquest.com/lib/kutu/detail.action?docID=3566938

[81] D. M. Mattox, "5. Thermal Evaporation and Deposition in Vacuum," in *Foundations of Vacuum Coating Technology (2nd Edition)*, Elsevier. [Online]. Available: https://app.knovel.com/hotlink/pdf/id:kt011PD368/foundations-vacuum-coating/thermal-evaporation-deposition

[82] J. Valdez García *et al.*, "Simplifying perovskite solar cell fabrication for materials testing: how to use unetched substrates with the aid of a three-dimensionally printed cell holder," *R Soc Open Sci*, vol. 11, no. 9, Sep. 2024, doi: 10.1098/rsos.241012.

[83] E. von Hauff and D. Klotz, "Impedance spectroscopy for perovskite solar cells: characterisation, analysis, and diagnosis," *J Mater Chem C Mater*, vol. 10, no. 2, pp. 742–761, 2022, doi: 10.1039/D1TC04727B.

[84] Y. Li, M. Cheng, E. Jungstedt, B. Xu, L. Sun, and L. Berglund, "Optically Transparent Wood Substrate for Perovskite Solar Cells," *ACS Sustain Chem Eng*, vol. 7, no. 6, pp. 6061–6067, Mar. 2019, doi: 10.1021/acssuschemeng.8b06248.

[85] K. Miettunen *et al.*, "Bio-based materials for solar cells," *WIREs Energy and Environment*, vol. 13, no. 1, Jan. 2024, doi: 10.1002/wene.508.

[86] L. Wågberg, G. Decher, M. Norgren, T. Lindström, M. Ankerfors, and K. Axnäs, "The Build-Up of Polyelectrolyte Multilayers of Microfibrillated Cellulose and Cationic Polyelectrolytes," *Langmuir*, vol. 24, no. 3, pp. 784–795, Feb. 2008, doi: 10.1021/la702481v.

[87] Z. Fang *et al.*, "Highly transparent paper with tunable haze for green electronics," *Energy Environ. Sci.*, vol. 7, no. 10, pp. 3313–3319, 2014, doi: 10.1039/C4EE02236J.

[88] L. Hu *et al.*, "Transparent and conductive paper from nanocellulose fibers," *Energy Environ. Sci.*, vol. 6, no. 2, pp. 513–518, 2013, doi: 10.1039/C2EE23635D.

[89] Z. Fang *et al.*, "Novel Nanostructured Paper with Ultrahigh Transparency and Ultrahigh Haze for Solar Cells," *Nano Lett*, vol. 14, no. 2, pp. 765–773, Feb. 2014, doi: 10.1021/nl404101p.

[90] F. Azzam, C. Moreau, F. Cousin, A. Menelle, H. Bizot, and B. Cathala, "Cellulose Nanofibril-Based Multilayered Thin Films: Effect of Ionic Strength on Porosity, Swelling, and Optical Properties," *Langmuir*, vol. 30, no. 27, pp. 8091–8100, Jul. 2014, doi: 10.1021/la501408r.

[91] C. N. Wu, T. Saito, S. Fujisawa, H. Fukuzumi, and A. Isogai, "Ultrastrong and high gas-barrier nanocellulose/clay-layered composites," *Biomacromolecules*, vol. 13, no. 6, pp. 1927–1932, Jun. 2012, doi: 10.1021/bm300465d.

[92] L. Li, L. Maddalena, Y. Nishiyama, F. Carosio, Y. Ogawa, and L. A. Berglund, "Recyclable nanocomposites of well-dispersed 2D layered silicates in cellulose nanofibril (CNF) matrix," *Carbohydr Polym*, vol. 279, p. 119004, Mar. 2022, doi: 10.1016/j.carbpol.2021.119004.

[93] X. Yang, L. Li, Y. Nishiyama, M. S. Reid, and L. A. Berglund, "Processing strategy for reduced energy demand of nanostructured CNF/clay composites with tailored interfaces," *Carbohydr Polym*, vol. 312, p. 120788, Jul. 2023, doi: 10.1016/j.carbpol.2023.120788.

[94] S. Castro-Hermosa, M. Top, J. Dagar, J. Fahlteich, and T. M. Brown, "Quantifying Performance of Permeation Barrier—Encapsulation Systems for Flexible and Glass-Based Electronics and Their Application to Perovskite Solar Cells," *Adv Electron Mater*, vol. 5, no. 10, 2019, doi: 10.1002/aelm.201800978.

[95] B. E. Droguet *et al.*, "Large-scale fabrication of structurally coloured cellulose nanocrystal films and effect pigments," *Nat Mater*, vol. 21, no. 3, pp. 352–358, Mar. 2022, doi: 10.1038/s41563-021-01135-8.

[96] J. Valdez Garcia *et al.*, "Multifunctional nanocellulose hybrid films: From packaging to photovoltaics," *Int J Biol Macromol*, vol. 292, p. 139203, Mar. 2025, doi: 10.1016/j.ijbiomac.2024.139203.

[97] A. Anand, M. M. Islam, R. Meitzner, U. S. Schubert, and H. Hoppe, "Introduction of a Novel Figure of Merit for the Assessment of Transparent Conductive Electrodes in Photovoltaics: Exact and Approximate Form," *Adv Energy Mater*, vol. 11, no. 26, Jul. 2021, doi: 10.1002/aenm.202100875.

[98] N. Nasiri, H. E. Cainglet, G. Garnier, and W. Batchelor, "Transparent maltitol- cellulose nanocrystal film for high performance barrier," *Cellulose*, vol. 31, no. 12, pp. 7421–7436, Aug. 2024, doi: 10.1007/s10570-024-06022-4.

[99] J. J. Benitez *et al.*, "Transparent, plasticized cellulose-glycerol bioplastics for food packaging applications," *Int J Biol Macromol*, vol. 273, p. 132956, Jul. 2024, doi: 10.1016/j.ijbiomac.2024.132956.

[100] J. A. Diaz, X. Wu, A. Martini, J. P. Youngblood, and R. J. Moon, "Thermal expansion of self-organized and shear-oriented cellulose nanocrystal films," *Biomacromolecules*, vol. 14, no. 8, pp. 2900–2908, Aug. 2013, doi: 10.1021/bm400794e.

[101] B. Guo, W. Chen, and L. Yan, "Preparation of Flexible, Highly Transparent, Cross-Linked Cellulose Thin Film with High Mechanical Strength and Low Coefficient of Thermal Expansion," *ACS Sustain Chem Eng*, vol. 1, no. 11, pp. 1474–1479, Nov. 2013, doi: 10.1021/sc400252e.

TURUN
YLIOPISTO
UNIVERSITY
OF TURKU

Grano, Turku, Finland 2026

ISBN 978-952-02-0522-5 (print)
ISBN 978-952-02-0523-5 (pdf)
ISSN 2736-9390 (print)
ISSN 2736-9684 (online)